GEAR TECHNOLOGY

The Journal of Gear Manufacturing

NOVEMBER/DECEMBER 1986

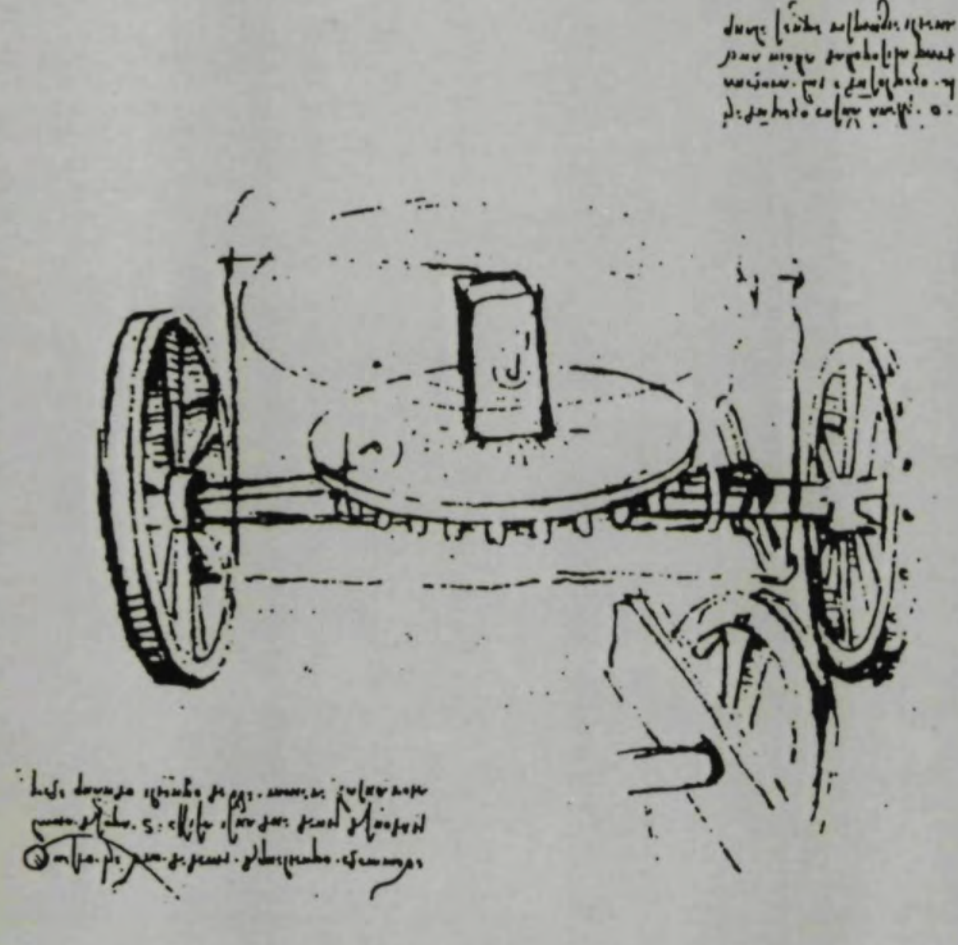

Kinematic Analysis of Robotic Bevel-Gear Trains

Mirror Finishing of Tooth Surfaces With A CBN Wheel

A Logical Procedure To Determine Gear Size

Curvic® Coupling Design


AMERICAN PFAUTER
MAAG
ZURICH
LORENZ
ETTLINGEN
KAPP

Who Says Quality Has to Cost More?
We Don't!

New Angle Gear produces precision, hard finished spiral bevel gearing, at cut and lapped prices.

Utilizing the Klingelnberg HPG-S method, state-of-the-art equipment delivers spiral bevel gears up to 30 inches diameter, at AGMA Levels 10-13. And New Angle gears accommodate higher loads (torque) with "whisper" quiet operation. Or. . . you may opt to reduce gear size to further reduce cost.

Also, matched sets are a thing of the past with our process of proven repeatability.

Our FREE quick facts brochure can tell you a lot more. . . Write or Call:

NEW ANGLE GEAR
King of Prussia, PA 19406
Phone: (215) 337-5400

CIRCLE A-3 ON READER REPLY CARD

RANDALL PUBLISHING
1401 Lunt Avenue
P.O. Box 1426
Elk Grove, IL 60007
(312) 437-6604

TYPOGRAPHY:
Kenric Graphics, Inc.
Elk Grove Village, IL

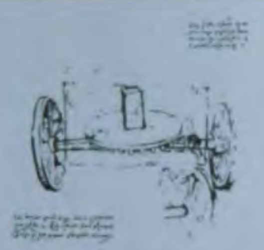

THE ADVANCED
OUR COVER

Vehicles of all kinds were the subject of many studies by Leonardo da Vinci. He did sketches of all sorts of conveyances from armored cars to horseless carriages. Our cover this month shows one of Leonardo's renditions of a transmission unit for the axle of a wagon. The large, toothed horizontal wheel turns the axle many times for each of its own revolutions, converting a slow action by the prime mover into a faster one at the cart wheels themselves. This design of a transmission system with a multiplying ratio is similar to one he used for millstones, with the addition of a handbrake.

GEAR TECHNOLOGY
The Journal of Gear Manufacturing

CONTENTS — PAGE NO.

November/December 1986 — Vol. 3, No. 6

GEAR TECHNOLOGY, The Journal of Gear Manufacturing (ISSN 0743-6858) is published bimonthly by Randall Publishing Co., Inc., 1425 Lunt Avenue, P. O. Box 1426, Elk Grove Village, IL 60007. GEAR TECHNOLOGY, The Journal of Gear Manufacturing is distributed free of charge to qualified individuals and firms in the gear manufacturing industry. Subscription rates for non-qualified individuals and firms are: $30.00 in the United States, $50.00 for foreign countries. Second-Class postage paid at Arlington Heights, IL and at additional mailing office.

Postmaster: Send address changes to GEAR TECHNOLOGY, The Journal of Gear Manufacturing, 1425 Lunt Avenue, P. O. Box 1426, Elk Grove Village, IL 60007.

MANUSCRIPTS: We are requesting technical papers of every sort from manufacturers of gear making machinery and related equipment, universities, and engineers. Articles should be of an educational and training nature with general appeal to anyone having anything to do with the purchase of materials or machinery, or the design, manufacture, testing or processing of gears. Subjects sought are solutions to specific problems, explanations of new: technology, techniques, designs, processes, and alternative manufacturing methods. These can range from the "How to . . ." of gear cutting (BACK TO BASICS) to the most advanced technology. All manuscripts submitted will be carefully considered. However, the Publisher assumes no responsibility for the safety or return of manuscripts. Manuscripts must be accompanied by a self-addressed, self-stamped envelope, and be sent to GEAR TECHNOLOGY, The Journal of Gear Manufacturing, P.O. Box 1426, Elk Grove, IL 60007, (312) 437-6604.

Before you buy a CNC Gear Inspection System, ask these four questions

1. Can we get complete inspection of both gears and cutting tools?

With the M & M 2000 QC System, the answer is yes. The system will test lead and involute profile characteristics of internal or external gears and splines. It is the only universal gear tester available which provides true index testing without expensive attachments. In addition, *we have fully-developed software for checking hobs, shaver* cutters, shaper cutters, and other cylindrical parts such as worms and cams.

Hob Pressure Angle Check

Shaver Cutter Lead Check

2. Can you customize software to meet our quality-inspection specifications?

At M & M Precision, we write and develop our own inspection software. Our technical team can and has implemented inspection specifications into specific software for individual requirements. Our current library includes line/curve fitting as well as modified K-chart analysis routines.

Line/Curve Fitting

Modified K-Chart Analysis

3. OK, you can inspect gears and cutting tools. What else is available to aid us in quality control of the manufacturing process?

At M & M Precision, we have fully integrated such advanced software packages as Statistical Process Control and Tooth *Topography into our standard testing software. Our SPC pro*gram can identify non-random variations and provide early warning of variations which are approaching tolerance limits. Our Tooth Topography software features automatic testing of lead and involute at multiple locations and provides two- and three-dimensional graphics.

SPC Run Chart

Topological Map

4. Do you have the technical support team and installation experience to back up the hardware and software provided?

At M & M Precision, we have a technical team with over 45 *man-years of experience in developing CNC gear inspection* hardware and software. All software for our QC 2000 System has been developed in-house. In addition, we have working installations at these leading companies:

- General Motors
- TRW
- Ford Motor
- Warner Gear
- Cincinnati Milacron
- Chrysler
- Pratt & Whitney
- Rocketdyne

For details on our advanced QC 2000 System and available software, contact M & M Precision Systems, 300 Progress Road, West Carrollton, Ohio 45449, 513/859-8273.

M&M PRECISION SYSTEMS

AN ACME-CLEVELAND COMPANY

CIRCLE A-6 ON READER REPLY CARD

EDITORIAL

THE COMPETITIVE EDGE

Now that the new tax bill has been passed, the time has come to begin evaluating how it will affect investment strategies in the machine tool business. Your first reaction may be to think that any motivation to invest in capital improvements in your company is gone, because both the investment tax credit and the accelerated depreciation on capital investment have been removed from the tax law. After all, if Uncle Sam is not going to help us out through some short term tax gains, why should we bother? Can we afford to bother?

The old tax laws did provide certain incentives, and their demise will require all of us to rethink our investment strategies carefully; however, it is self-defeating to assume that now that the tax breaks are gone, so is any reason to reinvest in our companies. The question is, can we afford *not* to invest in the latest, most advanced capital equipment we can, regardless of any changes in tax law.

Having just returned from IMTS, I am more aware than ever of the exciting and rapid changes occurring every day in machine tool technology. The company that does not keep up will, inevitably, be left behind. Maintaining one's competitive edge is also the best way to take advantage of some of the breaks that have been written into the new tax code. The dropping of the over-all corporate tax rate tends to offset the deletion of tax incentives for investment, *but only for companies that remain profitable*. Ultimately, an investment in the best, most advanced machinery a company can afford is its investment in maintaining its profits.

Undeniably, the newest technology is expensive. Current economic conditions are unsettled, and certain, comforting old tax breaks are gone. But, equally undeniably, the advent of CNC gear manufacturing equipment has given the industry a kind of flexibility in production never dreamed possible a few years ago; a flexibility that can provide a crucial competitive edge. For example, a past customer of ours, working in the oil field industry, bought a CNC gear hobber, even though he was not convinced he needed the CNC capability for his purposes. Then the bottom fell out of the oil industry. Now the "extras" he didn't think he needed give him the capability to economically produce small quantities of gears at a low cost because his set-up time is so much faster than it was on his older, manual machines. His CNC machine provides him with lower manufacturing costs, better utilization of his plant and less money tied up in finished inventory, at a time when he desperately needs those advantages to weather the economic storm.

Advanced technology provides manufacturers with economic and competitive advantages they cannot easily do without in today's world marketplace. In such a situation, to stay in the same place is to fall behind. Tax breaks or no tax breaks, we each must ask ourselves the question, "Can I afford not to invest in the future of my company?"

Michael Goldstein
Editor/Publisher

GUEST EDITORIAL

BALANCE IS CRITICAL—MONITORING ESSENTIAL

These are changing times for industry. Trauma and uncertainty are always a part of change, and change is not always for the better. Change is usually forced, most frequently by competition. Our competitive free enterprise system *should* be able to respond to competition because that's its basis. These are critical years. If we do not respond effectively to change and competition, it could be disasterous.

E. J. Campbell, President and CEO of Newport News Shipbuilding, in his Rentschler Memorial Lecture at the Tenth Annual Meeting of the Iron Castings Society, has addressed these same issues. Some of his thoughts are worthy of repeating and commenting on. Mr. Campbell calls for "individual and national resolve" to meet the challenge of competitiveness, which, he says, will be the economic agenda for the next decade. His call to action, while surely essential, is quite broad and leaves most of us with the feeling that the job is so big that it must be someone else's.

This writer feels much more comfortable discussing technology itself rather than the strategies and policies concerning its influence on the well-being of firms and, thus, the nation. However, it's time that technical people in industry take a broader view and enlarge their sphere of influence. Although Campbell's address does not discuss technology, it's quite easy to visualize improved generation and utilization of technology as a part of the "resolve" he says is essential. As a matter of fact, some changes are already in motion. Given our many special interest groups, though, to get agreement on action plans is most difficult.

On an *a priori* basis, it's easy to see the relationship between technology generation and utilization and progress. The problem comes in establishing priorities and balance, as, for example, in the areas of basic vs applied or "bread and butter research," the kind that sometimes parallels development programs for the purpose of providing answers so that development can continue. My concern at this moment has to do with some of the shifts that are taking place in this balance. Many firms are reducing their technical capabilities drastically. This has been common practice for decades during times of economic distress. Then, when times improve, there is usually a return to an emphasis on technical development. Unfortunately, foreign competition is such that the future doesn't look promising, so comeback in terms of technology utilization and generation in industry is not apt to happen. On the other hand, government laboratories and universities, with the aid of tax dollars, are redirecting their activities to try to help industry, so an effort *is* being made which may help fill the gap.

It is difficult to be critical and not sound negative, but we do need to continually, objectively monitor these kinds of changes and assess their value. What about the change we have just discussed; i.e., the shrinkage of research by industry and the expansion of it by entities normally engaged in more basic research? Will the new "research" be in synch with industry's needs? Will it be done efficiently and with a sense of urgency? Measuring the quality of research is difficult if its objectives aren't clear. For instance, if the objective is to generate a doctoral thesis or a publication, the research may not serve the needs of an industry operating in a survival mode. On the other hand, a research program which serves that need may not meet the criteria required for educational purposes. Many historians and analysts of technology are in agreement that the advance of technical knowledge depends on a system in which universities, industries, and government make demands on each other and cross-fertilize each other to meet those demands. We expect ASME-GRI to be actively participating in this arena. The management of ASME-GRI is dedicated to the promotion of both basic and applied research and to being sensitive to the necessary balances between them.

Two things are certain. All we technologists need an increased awareness concerning what's going on in both industry and in research and a resolve to participate unselfishly in order to maintain the balance that will aid our domestic industry retain its competitive edge.

Dale Breen, Director
ASME Gear Research Institute

DALE BREEN *is the director of ASME's Gear Research Institute. He has a master's degree in metallurgy from the University of Michigan and a MBA from the University of Chicago. He is a member of the American Society of Mechanical Engineers, the Society of Automotive Engineers, the American Society of Lubrication Engineers, the American Institute of Mining and Metallurgical Engineers and an American Society of Metals Fellow. Mr. Breen is co-author of the book,* Hardenability of Steel *and author of a chapter in* Fatigue and Microstructure, *as well as numerous shorter articles on gears, metallurgy and fatigue.*

Kinematic Analysis of Robotic Bevel-Gear Trains

F. Freudenstein
R. W. Longman
C.-K. Chen
Columbia University—New York, NY

Introduction

In robot configurations it is desirable to be able to obtain an arbitrary orientation of the output element or end-effector. This implies a minimum of two independent rotations about two (generally perpendicular) intersecting axes. If, in addition, the output element performs a mechanical task such as in manufacturing or assembly (e.g., drilling, turning, boring, etc.) it may be necessary for the end-effector to rotate about its axis. If such a motion is to be realized with gearing, this necessitates a three-degree-of-freedom, three-dimensional gear train, which provides a mechanical drive of gyroscopic complexity; i.e., a drive with independently controlled inputs about three axes corresponding to azimuth, nutation, and spin.

In a recent article[2] an ingenious bevel-gear train of this type was described, and the article refers to a project headed by Mr. Louis Erwin, Project Coordinator of the Bendix Corporation's Robotics Division, Southfield, Michigan, for the motion of the end-effector of a heavy-duty industrial robot (ML-360).

In this gear train, the orientation of the tool-carrying end-effector is determined by independent rotations about mutually perpendicular, intersecting axes in space, such as occur in the two-gimbal mounts of gyroscopes. In addition, the end-effector can rotate independently about its own axis. In such gear trains the gears and arms rotate about nonparallel axes, *which may themselves be rotating about other nonparallel* axes.

Various methods for deriving the displacement equations for spur-gear trains can be found in the literature.[1, 3, 6, 7, 8, 9] For these the most systematic approach utilizes the fundamental circuits (obtained directly from the graph of the gear train) from which the displacement equations follow automatically. In bevel-gear trains the analysis is more complex because of the three-dimensional motion of the gears and arms. When arm motion is limited to a rotation about a fixed axis, the displacement equation associated with a fundamental circuit and given in Ref.[4] should be used. In complex epicyclic bevel-gear trains, however, the fundamental circuit equations can no longer be reduced to scalar form, and one would need to monitor the paths of all moving axes, as well as gear and arm rotations. In the following sections a general method for the kinematic analysis of such trains will be developed; first with reference to the previously mentioned robotic bevel-gear train, and thereafter for bevel-gear trains of arbitrary complexity.

Kinematic Analysis of a Three-Degree-of-Freedom Robotic Gear Train (Fig. 1)

(1) *Kinematic Structure of Gear Train.* The gear train described in, Ref.[2], which is shown in cross section in Fig. 1, has three coaxial input rotations (the rotations of shafts 1, 2, 3 relative to the frame 4). Bevel-gears 1, 2, 5, 6, 7 transmit these rotations to the end-effector attached to gear 7 and housed in arm 8, which pivots on shaft 3. The axis locations of the turning pairs are as follows:

Axis a: pairs 1-2, 2-4, 4-3
Axis b: pairs 3-5, 3-8, 3-6
Axis c: pair 8-7

AUTHORS:

DR. FERDINAND FREUDENSTEIN *is Higgins Professor of Mechanical Engineering at Columbia University. Besides his academic activities, he has been active in consulting work to industry. His research interests include mechanisms, kinematics, dynamics, and design analysis. Dr. Freudenstein is a member of ASME, the National Academy of Engineering, Harvard Engineering Society, the Columbia Engineering Society and numerous other professional and honorary societies. He has authored over 130 publications and holds nine patents/invention disclosures. He is the winner of numerous professional and academic awards.*

R.W. LONGMAN *is on the faculty of Columbia University, doing research in control and dynamics as related to spacecraft and robotics. He also serves on the Board of Directors of the American Astronautical Society and is Managing Editor of their* Journal of the Astronautical Sciences. *He has been visiting professor at MIT, University of Bonn (West Germany), Newcastle (Australia) and Cheng Kung (Taiwan). In addition to his academic work, he has served as a consultant to a number of major corporations and defense contractors. He is a Fellow of the American Astronautical Society and an Associate Fellow of AIAA.*

C.-K. CHEN *received his Bachelor of Science Degree from National Taiwan University and his Master of Science from Columbia University. He is presently a graduate research assistant at Columbia, working primarily in the area of mechanisms.*

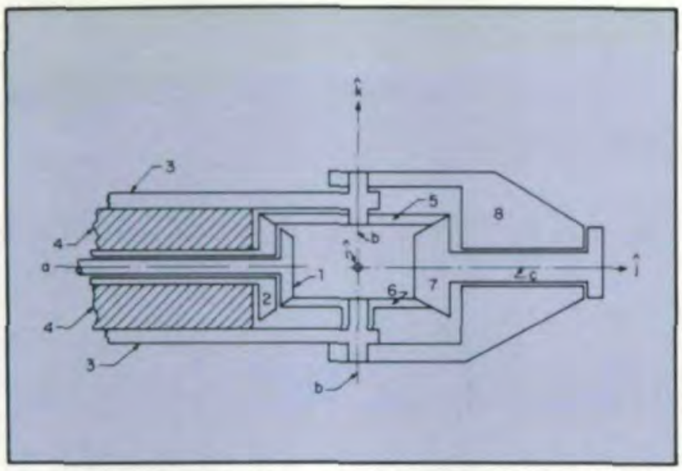

Fig. 1 – Cross section of robotic gear train shown in [2]; "initial" position of gear train

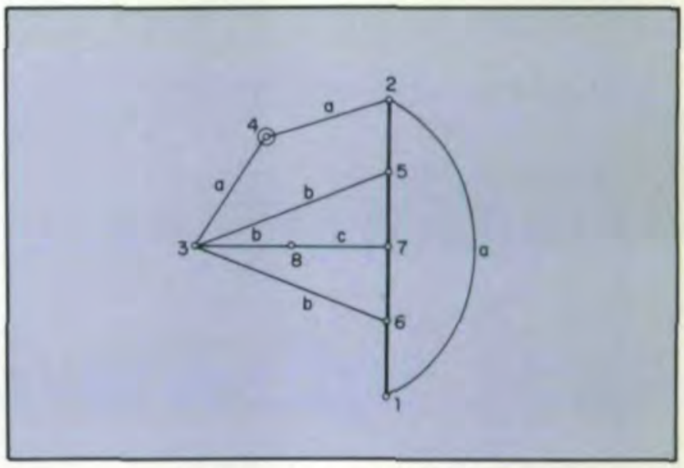

Fig. 2 – Graph of gear train of Fig. 1

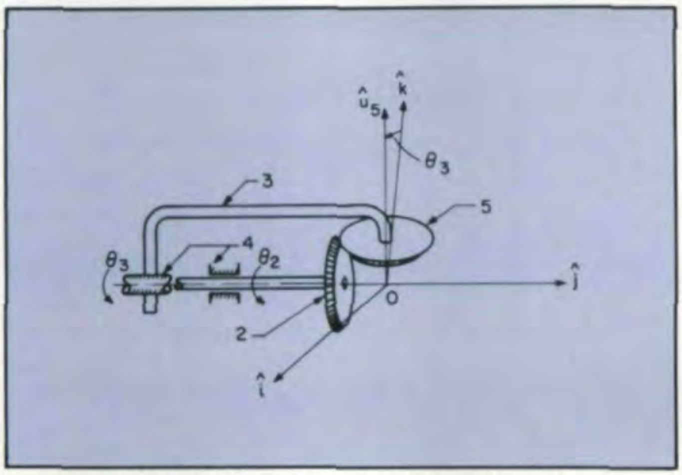

Fig. 3 – Fundamental circuit (2,5)(3) – schematic

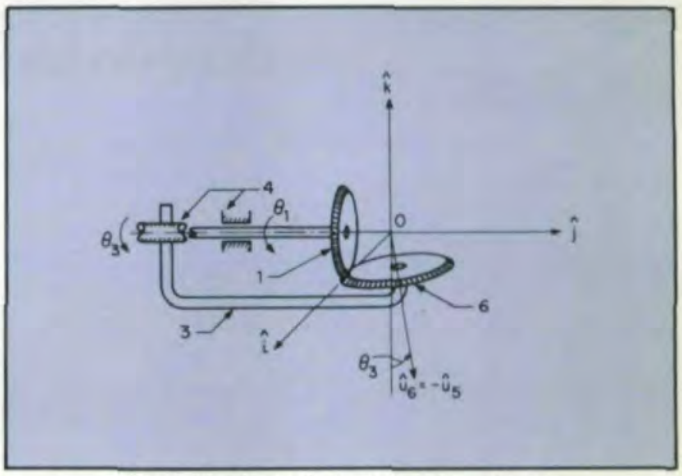

Fig. 4 – Fundamental circuit (1,6)(3) – schematic

The graph of the gear train (in which links are represented by vertices, joints by edges, and the edge connection of vertices corresponds to the joint connection of links) is shown in Fig. 2, in which light edges denote turning pairs and heavier edges denote gear pairs. As can be seen from the graph, the gear train has 8 links, 11 joints (4 gear pairs and 7 turning pairs). The mobility number of the spherical gear train is $\lambda = 3$. The degree of freedom, F, of the gear train is obtained from the equation:

$$F = \lambda(l - j - 1) + \Sigma f_i \tag{1}$$

where l, j, f_i denote the number of links, joints and freedom of the ith joint, respectively. This yields $F = 3(8 - 11 - 1) + 15 = 3$.

From the graph we observe that there are four fundamental circuits: (1,6)(3); (2,5)(3); (6,7)(8); and (5,7)(8). In this notation the first two numbers for each circuit designate the gears, and the last identifies the arm. One special feature of this gear train is evident at this point: since the pitch cones of the gears form a closed configuration, and the angle between the axes of any gear pair is the same (a right angle), it follows that the semi-vertex angle of the pitch cones alternates between complementary values (α, say, and, (90 deg $- \alpha$)).

We begin the analysis with the displacement equations associated with each fundamental circuit.

(2) *Fundamental Circuit (2,5)(3).* The fundamental circuit is shown in Fig. 3, including rotations θ_2, θ_3 of shafts 2 and 3, respectively. The positive direction of rotation of shafts 1, 2, and 3 corresponds to a right-handed rotation associated with the unit vector, $\hat{j}$, of the fixed, right-handed, orthogonal triad ($\hat{i}$, $\hat{j}$, $\hat{k}$). The direction of the axis of gear 5 is denoted by the outwardly drawn unit vector, $\hat{u}_5$, and point 0 is the point of intersection of the pitch cones of the gears.

The direction of vector $\hat{u}_5$ is given by

$$\hat{u}_5 = \cos\theta_3 \hat{k} + \sin\theta_3 \hat{i} \tag{2}$$

The angular displacements associated with the fundamental circuit are derived in Table 1 in terms of the tabular method (sum of displacements with and relative to arm). The number of teeth on gear i is denoted by N_i. The vectorial nature of the displacements is evident from the table.

(3) *Fundamental Circuit (1,6)(3).* The fundamental circuit, including the rotation, θ_1, of shaft 1, is shown in Fig. 4. The direction of the axis of gear 6 is denoted by the outwardly drawn unit vector, $\hat{u}_6$, where $\hat{u}_6 = - \hat{u}_5$. The

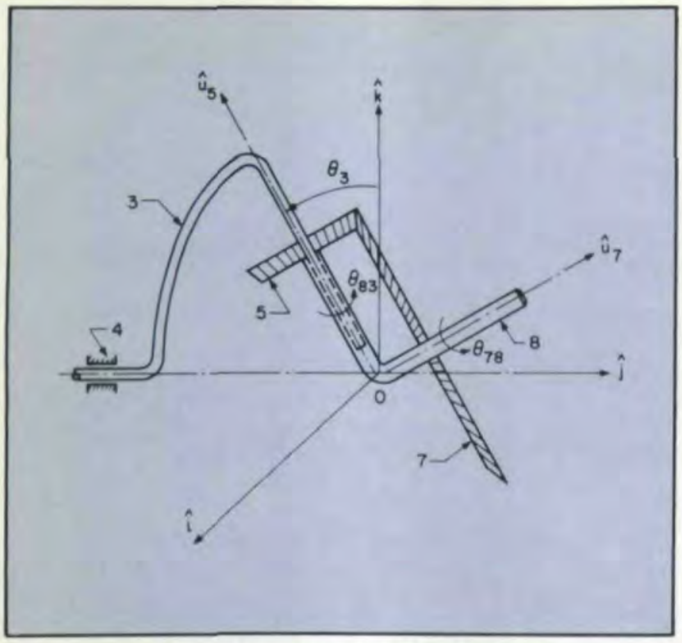

Fig. 5 – Fundamental circuit (5,7)(8) – schematic

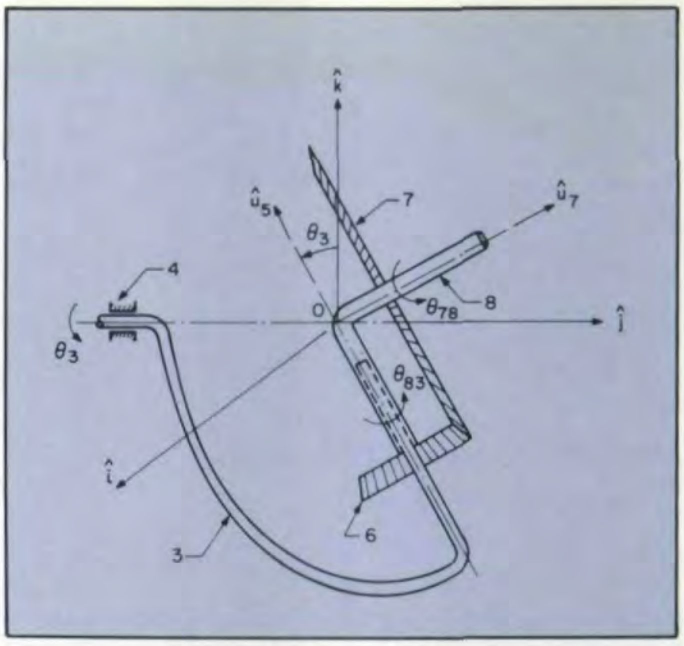

Fig. 6 – Fundamental circuit (6,7)(8) – schematic

angular displacements in this circuit are summarized in Table 2.

(4) *Fundamental Circuit (5,7)(8).* The fundamental circuit is shown in Fig. 5, in which θ_{78} denotes the angular displacement of gear 7 relative to arm 8 (positive direction defined by a right-handed rotation about unit vector $\hat{u}_7$, the latter outwardly directed along the axis of gear 7); θ_{83} denotes the angular displacement of arm 8 relative to shaft 3 (positive direction defined by a right-handed rotation about unit vector $\hat{u}_5$). The angular displacements in this circuit are summarized in Table 3. These are functions of the unit vectors $\hat{u}_5$ and $\hat{u}_7$. The latter needs to be determined.

The initial position of arm 8 (see Fig. 1) was taken with its axis coincident with the j-axis. The final position of arm 8 is obtained by two successive rotations: a rotation of magnitude θ_{83} about the $\hat{k}$-axis, followed by a rotation of magnitude θ_3 about the $\hat{j}$-axis. A systematic way of determining the final position of vector $\hat{u}_7$ involves a double application of Rodrigues' equation, one form of which (see for example, F. M. Dimentberg[5]) is as follows:

$$\mathbf{r}' = \mathbf{r}\cos\phi + (1-\cos\phi)\,(\hat{u}\cdot\mathbf{r})\,\hat{u} + (\hat{u}\times\mathbf{r})\sin\phi \qquad (3)$$

In this equation $\mathbf{r}'$ denotes the final position of a vector, $\mathbf{r}$ (the origin of both vectors lying on the axis of rotation), rotating by an angle ϕ about an axis, the direction of which is that of unit vector $\hat{u}$.

For the first rotation $\mathbf{r} = \hat{j}$, $\phi = \theta_{83}$ and $\hat{u} = \hat{k}$. This gives

$$\mathbf{r}' = \hat{j}\cos\theta_{83} - \hat{i}\sin\theta_{83}.$$

For the second rotation, we have $\mathbf{r} = \hat{j}\cos\theta_{83} - \hat{i}\sin\theta_{83}$, $\phi = \theta_3$ and $\hat{u} = \hat{j}$. This gives:

$$\hat{u}_7 = \mathbf{r}' = -\sin\theta_{83}\cos\theta_3\,\hat{i} + \cos\theta_{83}\,\hat{j} + \sin\theta_{83}\sin\theta_3\,\hat{k} \qquad (4)$$

In applying Rodrigues' equation to an open-loop mechanism, such as a robot configuration, it is easiest to start with the open end (the end-effector) and proceed toward the base. In this way, the initial position of all axes is the initial or reference position of the axes (as shown in Fig. 1 for this particular gear train) and the total number of rotations which need to be computed is minimized. It is worth noting that

Table 1 Angular displacements in fundamental circuit (2,5)(3)*

Motion	Gear 2	Gear 5	Arm 3
(*a*) Motion with arm	$\theta_3\hat{j}$	$\theta_3\hat{j}$	$\theta_3\hat{j}$
(*b*) Motion relative to arm	$\theta_{23}\hat{j}$	$\frac{N_2}{N_5}\theta_{23}\hat{u}_5$	0
Sum (actual motion)	$(\theta_{23}+\theta_3)\hat{j}$ $=\theta_2\hat{j}$	$\theta_3\hat{j} + \frac{N_2}{N_5}\theta_{23}(\cos\theta_3\hat{k}+\sin\theta_3\hat{i})$	$\theta_3\hat{j}$

*In the tables θ_i denotes the angular displacement of gear i (relative to ground) and θ_{ij} the angular displacement of gear i relative to gear j (i.e., $\theta_{ij} = \theta_i - \theta_j$).

Table 2 Angular displacements in fundamental circuit (1,6)(3)

Motion	Gear 1	Gear 6	Arm 3
(*a*) Motion with arm	$\theta_3\hat{j}$	$\theta_3\hat{j}$	$\theta_3\hat{j}$
(*b*) Motion relative to arm	$\theta_{13}\hat{j}$	$\frac{N_1}{N_6}\theta_{13}\hat{u}_6$	0
Sum	$(\theta_{13}+\theta_3)\hat{j}$	$\theta_3\hat{j}-\frac{N_1}{N_6}\theta_{13}\hat{u}_5$	$\theta_3\hat{j}$
	$=\theta_1\hat{j}$	$=\theta_3\hat{j}-\frac{N_1}{N_6}\theta_{13}(\cos\theta_3\hat{k}+\sin\theta_3\hat{i})$	

Table 3 Angular displacements in fundamental circuit (5,7)(8)

Motion	Gear 5	Gear 7	Arm 8
(*a*) Motion with arm	$\theta_3\hat{j}+\theta_{83}\hat{u}_5$	$\theta_3\hat{j}+\theta_{83}\hat{u}_5$	$\theta_3\hat{j}+\theta_{83}\hat{u}_5$
(*b*) Motion relative to arm	$\frac{-N_7}{N_5}\theta_{78}\hat{u}_5$	$\theta_{78}\hat{u}_7$	0
Sum	$\theta_{13}\hat{j}+\left(\theta_{83}-\frac{N_7}{N_5}\theta_{78}\right)\hat{u}_5$	$\theta_3\hat{j}+\theta_{83}\hat{u}_5$ $+\theta_{78}\hat{u}_7$	$\theta_3\hat{j}+\theta_{83}\hat{u}_5$

Table 4 Angular displacements in fundamental circuit (6,7)(8)

Motion	Gear 5	Gear 7	Arm 8
(*a*) Motion with arm	$\theta_3\hat{j}$ $+\theta_{83}\hat{u}_5$	$\theta_3\hat{j}$ $+\theta_{83}\hat{u}_5$	$\theta_3\hat{j}$ $+\theta_{83}\hat{u}_5$
(*b*) Motion relative to arm	$\frac{N_7}{N_6}\theta_{78}\hat{u}_5$	$\theta_{78}\hat{u}_7$	0
Sum	$\theta_3\hat{j}+\left(\theta_{83}+\frac{N_7}{N_6}\theta_{78}\right)\hat{u}_5$	$\theta_3\hat{j}+\theta_{83}\hat{u}_5+\theta_{78}\hat{u}_7$	$\theta_3\hat{j}+\theta_{83}\hat{u}_5$

since only the relative motions at the joints is needed, the sequence of the finite rotations is immaterial (i.e., the rotation operations are commutative). The angular displacements of this circuit are summarized in Table 3.

(5) *Fundamental Circuit (6,7)(8).* This circuit is shown in Fig. 6 and the angular displacements are summarized in Table 4.

(6) *Compatibility Conditions.* In the angular displacements of the gears in the four fundamental circuits two gears (5 and 6) occur in two fundamental circuits: Gear 5 occurs in circuits (2,5)(3) and (5,7)(8); and gear 6 occurs in circuits (1,6)(3) and (6,7)(8). The angular displacements of each gear, as derived from the two circuits, can now be equated. These are the compatibility conditions which lead to the angular-displacement equations of the gear train.

From Tables 1 and 3, the compatibility condition for gear 5 is the following:

$$\frac{N_2\theta_{23}}{N_5}\sin\theta_3\hat{i}+\theta_3\hat{j}+\frac{N_2\theta_{23}}{N_5}\cos\theta_3\hat{k}$$
$$=\left(\theta_{83}-\frac{N_7}{N_5}\theta_{78}\right)\sin\theta_3\hat{i}+\theta_3\hat{j}+\left(\theta_{83}-\frac{N_7}{N_5}\theta_{78}\right)\cos\theta_3\hat{k} \tag{5}$$

where

$$\theta_{83}-\frac{N_7}{N_5}\theta_{78}=\frac{N_2\theta_{23}}{N_5} \tag{6}$$

Similarly, using Tables 2 and 4, the compatibility condition for gear 6 is:

$$-\frac{N_1}{N_6}\theta_{13}\sin\theta_3\hat{i}+\theta_3\hat{j}-\frac{N_1}{N_6}\theta_{13}\cos\theta_3\hat{k}$$
$$=\left(\theta_{83}+\frac{N_7}{N_6}\theta_{78}\right)\sin\theta_3\hat{i}+\theta_3\hat{j}+\left(\theta_{83}+\frac{N_7}{N_6}\theta_{78}\right)\cos\theta_3\hat{k} \tag{7}$$

where

$$-\frac{N_1}{N_6}\theta_{13}=\theta_{83}+\frac{N_7}{N_6}\theta_{78} \tag{8}$$

(7) *The Displacement Equations.* The angular-velocity ratio of a pair of bevel-gears, i, j, with semivertex angles α_i and α_j, respectively, and rotating about fixed axes with angular velocities w_i and w_j, respectively, is given by

$$\frac{\omega_i}{\omega_j}=\frac{\sin\alpha_i}{\sin\alpha_j} \tag{9a}$$

In view of the right angle between the axes of the gears, $\alpha_i = 90\text{ deg} - \alpha_j$, so that

$$\tan\alpha_j=\frac{\omega_i}{\omega_j}=\frac{N_j}{N_i} \tag{9b}$$

Hence, if α denotes the semivertex angle of the pitch cone of gear 1, it follows that

$$\tan\alpha=N_1/N_6=N_2/N_5 \tag{10a}$$

and that

$$1/\tan\alpha=N_6/N_7=N_5/N_7 \tag{10b}$$

Substituting equations (10*a*, *b*) into the compatibility equations (6) and (8), respectively, we have

$$-\theta_{78}\tan\alpha+\theta_{83}=\theta_{23}\tan\alpha \tag{11}$$

and

$$\theta_{78}\tan\alpha+\theta_{83}=-\theta_{13}\tan\alpha \tag{12}$$

This yields

$$\theta_{78}=-\frac{1}{2}(\theta_1+\theta_2-2\theta_3) \tag{13}$$

and

$$\theta_{83}=\frac{1}{2}(\theta_2-\theta_1)\tan\alpha \tag{14}$$

Substituting Equation 14 into Equation 4 for $\hat{u}_7$ we obtain the orientation of the end-effector, which is

$$\hat{u}_7=-\sin\left[\frac{1}{2}(\theta_2-\theta_1)\tan\alpha\right]\cos\theta_3\hat{i}$$
$$+\cos\left[\frac{1}{2}(\theta_2-\theta_1)\tan\alpha\right]\hat{j}$$
$$+\sin\left[\frac{1}{2}(\theta_2-\theta_1)\tan\alpha\right]\sin\theta_3\hat{k} \tag{15}$$

Equations 13-15 give the orientation of the end-effector and its angular displacement as a function of the rotations of the input shafts.

Discussion

The angular displacements of all gears as a function of input rotations follows directly from the tables with the aid of Equations 13-15. Equations 13-15 support the statements made in Ref.[2]. We find that:

(*a*) When the internal shafts 1 and 2 rotate equally in opposite directions, arm 8 pivots about the wrist axes of gears 5 and 6 and $\hat{u}_7 = \hat{j}$.

(*b*) If shafts 1 and 2 are stationary, the entire assembly rotates with shaft 3, the end-effector rotating at twice the speed of shaft 3.

(*c*) If shafts 1 and 2 rotate equally in the same direction, the end-effector rotates in its bearings in arm 8, the position of which is determined by shaft 3.

Variation of the pitch-cone semivertex angle, α, can serve to increase or decrease the magnitude of the angular displacements of the end-effector relative to those of the input shafts.

A General Procedure for the Kinematic Analysis of Complex Bevel-Gear Trains

In light of the analysis which has just been given a sequential, multi-step procedure applicable to the kinematic analysis of general, complex bevel-gear trains can be formulated as follows:

(*a*) Determine the graph (i.e., the kinematic structure) of the gear train, its degree of freedom and any special restrictions on dimensions (such as, the closure of the pitch cones).

(*b*) Determine the fundamental circuits of the gear train.

(*c*) Derive the angular-displacement equations for each fundamental circuit, keeping track not only of the arm and gear rotations, but also of the moving axes of these members. In the case of gear trains of gyroscopic complexity (i.e., gear trains in which one or more arms can rotate about two non-parallel, intersecting axes) the general displacement equations for a fundamental circuit are derived in the Appendix. In the

Table 5 Angular displacements of gears and arm in a fundamental circuit of gyroscopic complexity

Motion	Gear 1	Gear 2	Arm 3
(*a*) Motion with arm	$\theta\hat{k}$ $+\phi\hat{a}$	$\theta\hat{k}$ $+\phi\hat{a}$	$\theta\hat{k}$ $+\phi\hat{a}$
(*b*) Motion relative to arm	$\frac{N_2}{N_1}\psi\hat{a}$	$\psi\hat{s}$	0
Sum	$\theta\hat{k}+\left(\phi+\frac{N_2}{N_1}\psi\right)\hat{a}$	$\theta\hat{k}+\phi\hat{a}+\psi\hat{s}$	$\theta\hat{k}+\phi\hat{a}$

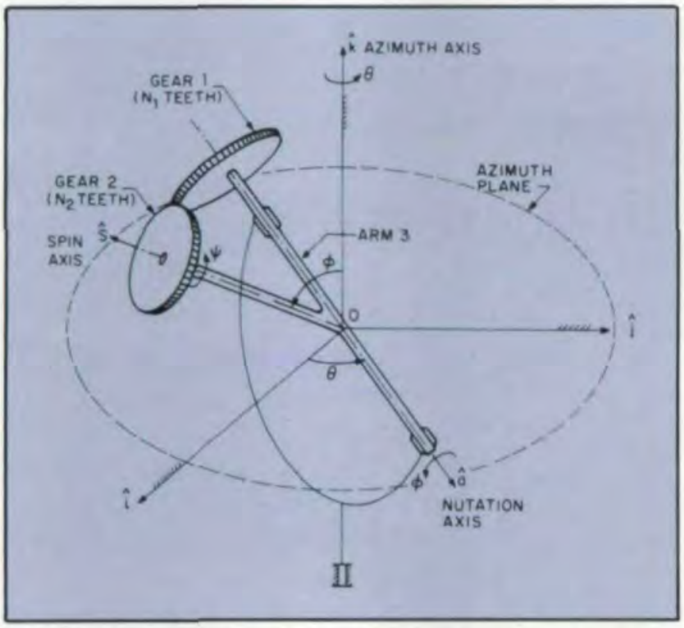

Fig. 7 – Fundamental circuit of a bevel-gear pair the motion of which is of gyroscopic complexity

case of gear trains of greater complexity (e.g., those in which the arm can rotate about an arbitrary number of nonparallel, intersecting axes), the fundamental-circuit equation can be derived generally along similar lines by means of the multiple application of Rodrigues' theorem.

(*d*) Determine the compatibility equations from the fundamental circuit equations.

(*e*) Determine the displacement equations from the compatibility equations.

Conclusion

The analysis of a robotic, three-degree-of-freedom bevel-gear train has been developed in detail and a general procedure outlined, which, with a multiple application of Rodrigues' theorem, yields a general and systematic procedure for the kinematic analysis of bevel-gear trains of arbitrary complexity, such as occur in three-dimensional applications, including robotics. The procedure can be readily computerized.

Appendix

The Displacement Equations for a Fundamental Circuit of a Bevel-Gear Pair in a Bevel-Gear Train of Gyroscopic Complexity. We consider the general circuit consisting of bevel-gears 1, 2, arm 3 and the gimbal mount of the arm, as shown in Fig. 7.

A fixed, right-handed, Cartesian coordinate system associated with unit vectors $\hat{i}$, $\hat{j}$, $\hat{k}$ and with $\hat{i}$, $\hat{j}$ in the horizontal (or azimuthal) plane is shown with origin at the point of intersection of the pitch cones of the bevel gears. The rotation of the arm is composed of the rotation, ϕ, about the nutation axis (directed along unit vector $\hat{a}$) and rotation, θ, about azimuth axis, $\hat{k}$. All rotations are defined in the right-handed sense about their respective axes. Gears 1 and 2 have N_1 and N_2 teeth, respectively, and the rotation of gear 1 relative to the arm about the spin axis (unit vector $\hat{s}$) is ψ. The azimuth, nutation, and spin axes are indicated in the figure.

The angular displacements of the gears and arm can be obtained by considering the motion relative to and with the arm, as given in Table 5. In addition, we need to keep track of the positions ($\hat{k}$, $\hat{a}$, $\hat{s}$) of the azimuth, nutation, and spin axes. Vector $\hat{k}$ is fixed, and vector $\hat{a}$ is given by:

$$\hat{a}=\cos\theta\hat{i}+\sin\theta\hat{j} \tag{A1}$$

Vector $\hat{s}$ is obtained from a double application of Rodrigues' equation.[3] In the first rotation $\mathbf{r}=\hat{k}$, $\phi=\phi$, $\hat{u}=\hat{i}$ and $\mathbf{r}'=\hat{k}\cos\phi-\hat{j}\sin\phi$; and in the second rotation $\mathbf{r}=\hat{k}\cos\phi-\hat{j}\sin\phi$, $\phi=\theta$ and $\hat{u}=\hat{k}$. This gives:

$$\hat{s}=\mathbf{r}'=\sin\phi\sin\theta\hat{i}-\sin\phi\cos\theta\hat{j}+\hat{k}\cos\phi \tag{A2}$$

Substituting equations (A1, A2) into the resultant displacements shown in Table 5, we obtain the angular displacements of the gears relative to the fixed unit triad ($\hat{i}$, $\hat{j}$, $\hat{k}$) as follows:

Position of gear 1:

$$\left(\frac{N_2}{N_1}\psi+\phi\right)\cos\theta\hat{i}+\left(\frac{N_2}{N_1}\psi+\phi\right)\sin\theta\hat{j}+\theta\hat{k} \tag{A3}$$

Position of gear 2:

$$(\phi\cos\theta+\psi\sin\phi\sin\theta)\hat{i}+(\phi\sin\theta-\psi\sin\phi\cos\theta)\hat{j}+(\theta+\psi\cos\phi)\hat{k} \tag{A4}$$

Position of arm 3:

$$\phi\cos\theta\hat{i}+\phi\sin\theta\hat{j}+\theta\hat{k} \tag{A5}$$

(continued on page 48)

Mirror Finishing of Tooth Surfaces Using A Trial Gear Grinder With Cubic-Boron-Nitride Wheel

by
A. Ishibashi, S. Ezoe, S. Tanaka
Saga National University, Japan

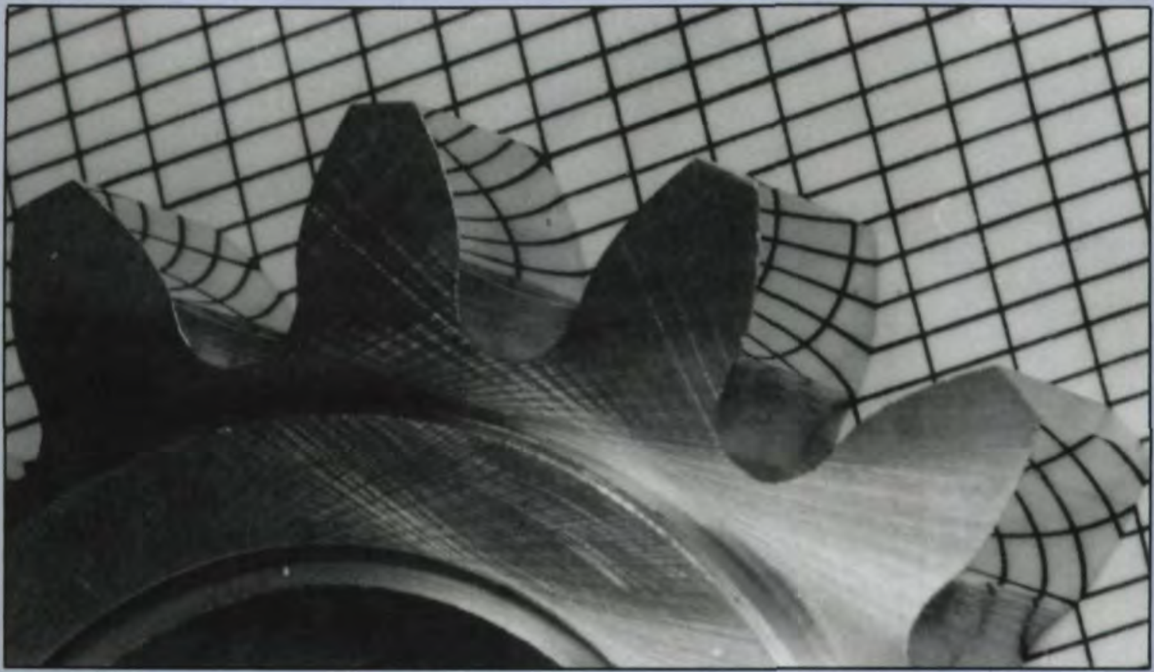

Fig. 1—Gear mirror finished by the authors' grinder

AUTHORS:

DR. AKIRA ISHIBASHI *is a Professor of Mechanical Engineering at Saga National University, Japan. He is also director of the university's Laboratory of Machine Design and Manufacturing Technique. Since 1959, his primary research interest has been in the area of gear manufacturing techniques and load carrying capacities, and he has published the results of his work in the Transactions of the Japan Society of Mechanical Engineers. He is a member of JSME, the Japan Society of Precision Engineering, The Japan Society of Lubrication Engineers, and the Society of Automotive Engineers of Japan, as well as several other professional organizations.*

DR. SHIGETADA TANAKA *is Associate Professor of Mechanical Engineering at Saga National University, Japan. He has been involved in research on the load carrying capacities of gears since 1966 and has developed a new gear grinder with a cubic-boron-nitride wheel. He is a member of the JSME, the Japan Society of Precision Engineering and the Japan Society of Lubrication Engineers.*

MR. SATORU EZOE *has a Bachelor of Engineering degree and is a Research Associate in the Department of Mechanical Engineering at Saga National University, Japan. His work has been mainly in the area of gear manufacturing techniques and load carrying capacities of precision gears. He is a member of the JSME, the Japan Society of Precision Engineering and the Japan Society of Lubrication Engineers.*

Introduction

In conventional gear grinders, grinding wheels with Alundum grains and a hardness of about 2000 HV have been used for finishing steel gears with hardnesses up to about 1000 HV. In this case, the accuracy of the gears ground is greatly affected by wear of the grinding wheel because the difference in hardness is comparatively small when the gears are fully hardened.

It is generally accepted that the wear of material becomes smaller when its hardness is greater. Diamond is the hardest of all materials; however, grinding wheels with diamond grains (HK = 6900 − 9600)[1] are not suitable for the finishing of steel gears with hardnesses in the range of 100 to 1000 HV. Although they can efficiently finish the tungsten carbide tools with a higher hardness of about 1800 HV. Diamond is more reactive with steel than with tungsten carbide at the high temperatures and pressures which occur in the grinding process. Therefore, chemical reaction and mechanical adhesion are likely to occur at the interface of the cutting edges of diamond grains and the virgin surface of steel, causing larger losses in the diamond wheel.

Grinding wheels with cubic-boron-nitride (CBN) grains have been used to sharpen high speed steel cutters with a hardness of about 850 HV[2] and for finishing hardened steels. The hardness of CBN grains is about 4600 HV,[6] appreciably lower than that of diamond grains. However, wear of wheels with CBN grains is appreciably smaller than wheels with diamond grains in the grinding of steels.

Recently, gear grinders with a CBN wheel have been developed for finishing hardened steel gears, and a remarkable reduction in the wear of the grinding wheel has been achieved,[3,4] as suggested by the results obtained from grinding flat surfaces and circular cylinders.[5,7] However, the tooth surfaces finished by CBN wheels were appreciably rougher than those finished by Alundum wheels. It was believed that CBN wheels never produce tooth surfaces with a peak-to-valley roughness less than 1.0 μm R_{max} ($\pm$ 10μ in. Ra). This has been the most important problem to solve in the development of gear grinders with a CBN wheel.

In contrast to earlier results,[3,7] the authors succeeded in remarkably decreasing the surface roughness of gear teeth and finally achieved mirror-like finishing using a trial gear grinder with a CBN wheel. Fig. 1 shows a mirror finished spur-gear with a module of 5. Crossed lines on the floor are clearly seen on the tooth surfaces of the gear.

In this article, the mechanism of mirror finishing with a CBN wheel will be explained, and then wear characteristics of CBN wheels used in mirror finishing of steel gears will be investigated by changing the speeds of the wheel and work, the depth of cut, the amount of grinding fluid, etc.

Trial Gear Grinder for Mirror-like Finishing

Mechanism of Gear Grinding and the Shape of the Wheel

It is very important to examine the basic mechanism of gear grinding and the shape of the grinding wheel which is most suitable for obtaining very smooth mirror-like tooth surfaces. The most important factor in obtaining the mirror-finished surfaces is the minimization of both the vibration of the grinding wheel and the clearance in the guide ways for the saddle on a work gear being ground. Moreover, the mechanism of the grinder must be simple in order to obtain a high accuracy gear grinder which can bring about accurately finished teeth with a very small surface roughness of about 0.1 μm R_{max}.

After some investigation, it was found that the geometrical shape of the CBN wheels used in the earlier experiments [3,4] are not suitable for the mirror finishing of tooth surfaces. When the disk-type grinding wheel with a trapezoidal section or the forming-type grinding wheel with an involute profile is used, most parts of the tooth surfaces, (i.e., the different parts of a tooth profile) will be finished by different abrasive grains located at the different positions. In this case, the height of a large number of the abrasive grains on the wheel must be in the narrow range, less than 0.2 μm, in order to obtain mirror finished surfaces. This is nearly impossible in practice, and, therefore, mirror-finished tooth surfaces will never be obtained when the disk-type and forming-type grinding wheels are used.

The few protruding grains on the CBN wheel are considered the enemy which prevents production of smoother surfaces. This is because the protruding grains scarcely wear due to the high wear resistance of CBN grains. After some investigation, however, the authors succeeded in effectively utilizing a few protruding CBN grains for mirror finishing of tooth surfaces by using a trial gear grinder designed and made by the authors.

Trial Gear Grinder with CBN wheel

Fig. 2 shows a schematic drawing of the trial gear grinder used in the mirror finishing of spur gears. The wheel spindle was rotated through a flat belt with a width of 40 mm at a rotational speed of about 1800 or 3600 rpm using an induction motor with a maximum output of 1.5 KW. The rolling motion for tooth profile generation was given by two pairs of steel bands and a cylinder with a diameter approximately equal to that of the base circle of the gear being ground.

For guiding the saddle with a work-gear mounting shaft, two cylinders and linear ball guide bushings were used under preloading conditions to avoid even the slightest run out (meandering motion) which might occur during tooth profile generation. The two pairs of angular ball bearings for the CBN wheel spindle shaft were preloaded to about 1000 N using eight coil springs of the same size. Fig. 3 shows the sectional view of the wheel spindle head.

Table 1 shows specifications of grinding wheels used in the present experiments. The Alundum wheels were used for comparison tests. Truing of the CBN wheels was done by a multi-grain type diamond dresser using an attachment shown in Fig. 4. After truing, the CBN wheels were dressed by an abrasive tip made of Alundum grains with vitrified bonds. Grinding was done with and without grinding fluid. Nonsoluble grinding fluid was used and flooded at a rate of 0.05 to 6.0 L/min.

Mechanism of Mirror Finishing by CBN Wheel

As shown in Fig. 2, a dish-type CBN wheel was used in the authors' grinder. Using this grinding wheel, plunge grinding in the direction of the wheel axis was done on a test

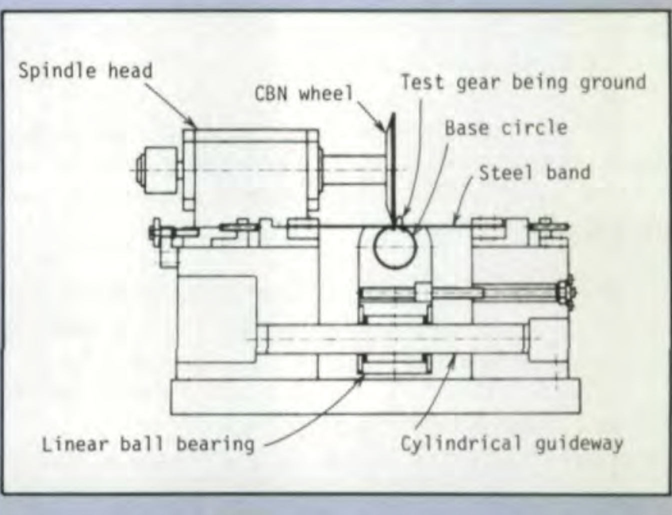

Fig. 2 – Schematic drawing of the grinder used for mirror finishing of tooth surface

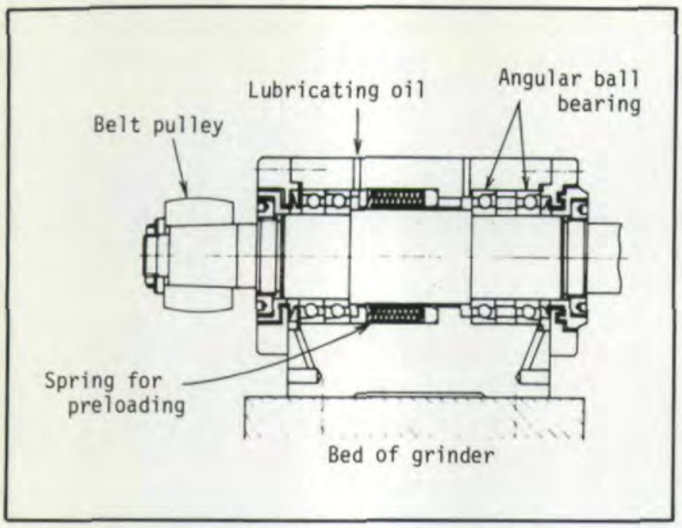

Fig. 3 – Sectional view of wheel spindle head

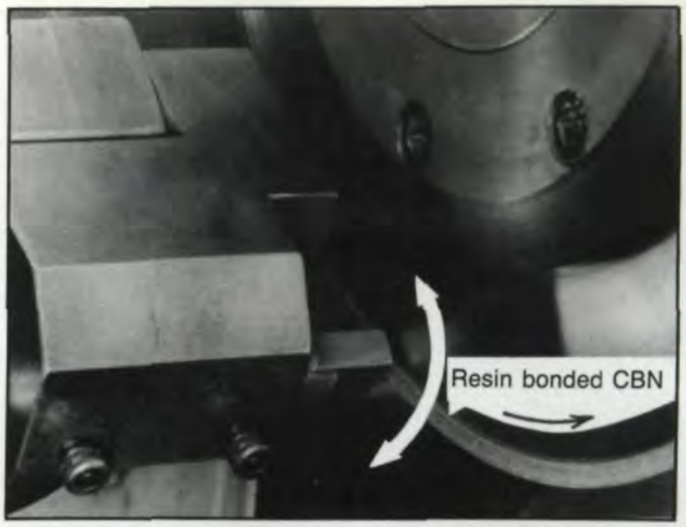

Fig. 4 – Attachment for truing of CBN wheel

TABLE 1—TYPES AND SPECIFICATIONS OF GRINDING WHEELS

Abrasive grain	Grain size	Grade	Concentration	Bond	Diameter
CBN	50	N	100	B	200 mm
	100	N	100	B	200 mm
	100	N	75	M	200 mm
	200	N	100	B	200 mm
Abrasive grain	**Grain size**	**Grade**	**Structure**	**Bond**	**Diameter**
WA	60	K	6	V	200 mm
	220	K	6	V	200 mm

specimen with a width of 5 mm, and then the ground surface was measured by a roughness meter to determine the effects of truing and dressing upon the ground surface. As supposed, it was impossible to obtain surface roughnesses less than 1.0 μm R_{max} even when careful truing was conducted using the multi-grain diamond tip. An example of the roughness of the plunge ground surface is shown in Fig. 5(a). From this figure we see that the surface roughness is about 1.5 μm R_{max} and agrees with the one generally supposed from earlier investigations.

However, surprisingly, the mirror finished surface with a roughness of about 0.1 μm R_{max} is obtained. Fig. 5(b) shows the same wheel used for generating tooth surfaces just after the plunge grinding.

Mirror Finishing by CBN Wheel With No Wear.

A roughness curve obtained from the plunge grinding is shown on the right side of Fig. 6. This curve indicates the envelope of the effective grains which participate in the final finishing of the plunge grinding. One of the valleys in the roughness curve may not be finished by the top of a single grain, but for the sake of simplicity, it is assumed that one valley is produced by one grain. In Fig. 6, Numbers 2′, 1′, 0, 1, 2, and 3 are given to the valleys of the roughness curve to indicate the tops of the effective grains in the plunge grinding.

In the case of generating grinding, only a few grains participate in final finishing and can bring about mirror finished surfaces if the gear grinder is properly designed, accurately made, and if the work feeding speed (rolling speed of base cylinder) is properly selected.

For example, when a CBN wheel which has produced a plunge ground surface with a roughness of about 1.5 μm R_{max} is used for generating tooth profiles of the test gear as shown Table 2, only grains 0, 1, and 2 participate in the final finishing of teeth as shown in Fig. 6. Only the grain "0" participates in the final finishing at the section (A - A), while the grain "1" does at the sections (B - B) and (B′ - B′). The three limited areas finished by the corresponding three grains 0, 1, and 2 are indicated in Fig. 6(a).

Mirror Finishing by CBN Wheel With Wear

When wear of a CBN wheel has occurred after grinding many teeth, the effective surface of the wheel deviates from a straight line, which is schematically shown on the right side of Fig. 7. The maximum wear at the edge of the wheel is 6 μm, and the height of effective grains is 2 μm, and their pitch is 0.1 mm. The calculated results indicate that the effective grains participating in final finishing are three in number as shown in Fig. 7(a).

In the case of the wheel with actual shape of wear pattern, similar results were obtained when the maximum wear, the height of effective grains and the pitch of the grains were nearly equal to those of the schematical shape of wear pattern. This result was supported by experiments in which mirror finished surfaces were obtained using a CBN wheel with wear.

Mirror Finished and Conventionally Finished Gears

Specifications of test gears used in the comparison tests are shown in Table 2. The hardness of test gears used for the following experiments was the same (800 HV) although some gears with different hardnesses were used for obtaining the grinding ratio.

Tooth Surface Roughness

Fig. 8 shows surface roughnesses of test gears finished by three different methods. The roughnesses were measured in the direction of tooth profile using a Talysurf roughness meter. Fig. 8(a) indicates the surface roughnesses of the test gear which was mirror finished by a CBN wheel using the trial gear grinder designed and made by the authors. Fig. 8(b) shows the surface roughnesses of the gear finished by a conventional precision gear grinder with an Alundum wheel. Fig. 8(c) shows the roughnesses of the gear finished on a precision hobbing machine with a carbide skiving-hob. It is evident from Fig. 8 that the surface roughness of the test gear finished by the authors' grinder is extremely small and is about 0.1 μm R_{max} (about 1.0 μ in. Ra).

Tooth Profile and Tooth Trace

Surface durability of gears cannot be increased sufficiently by a reduction in roughness of teeth alone. Accuracies of the tooth profile and the tooth trace must be increased at the same time. Figs. 9 and 10 show the tooth profiles and traces of test gears finished by three different methods. From these figures it may be seen that both the tooth profile and the tooth trace of the gear mirror finished by the authors' grinder are the best. This is because the mechanism of the grinder is very simple, resulting in an accurate generating motion.

Fig. 5 – Roughnesses of surface produced by CBN wheel

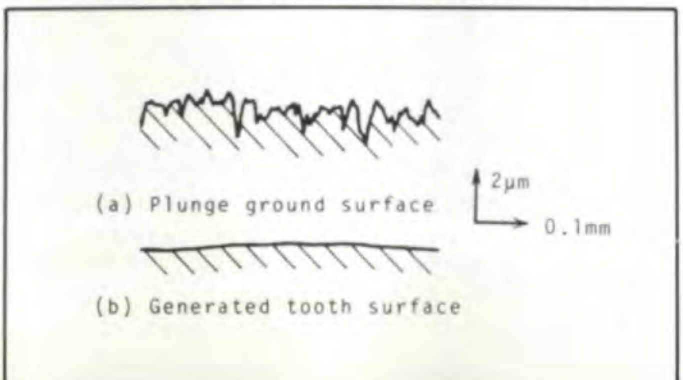

Conditions for Mirror Finishing

Effects of Grain Size and Wheel Speed

It is generally supposed that grinding wheels with a very small grain size are indispensable for obtaining mirror-finished surfaces. However, this supposition does not apply to the authors' grinder as can be understood from the mechanism

TABLE 2 – SPECIFICATIONS OF TEST GEARS

Module	m	3
Pressure Angle	α	20°
Number of teeth	Z	25
Face width	b	15 mm
Pitch circle dia.	d	75 mm
Outside dia.	d_K	81 mm
Helix angle	β	0°
Hardnesses (Materials)	800 Hv (SCM415) 290 HB (SCM435)	

Fig. 6 – Mechanism of mirror finishing by wheel with no wear

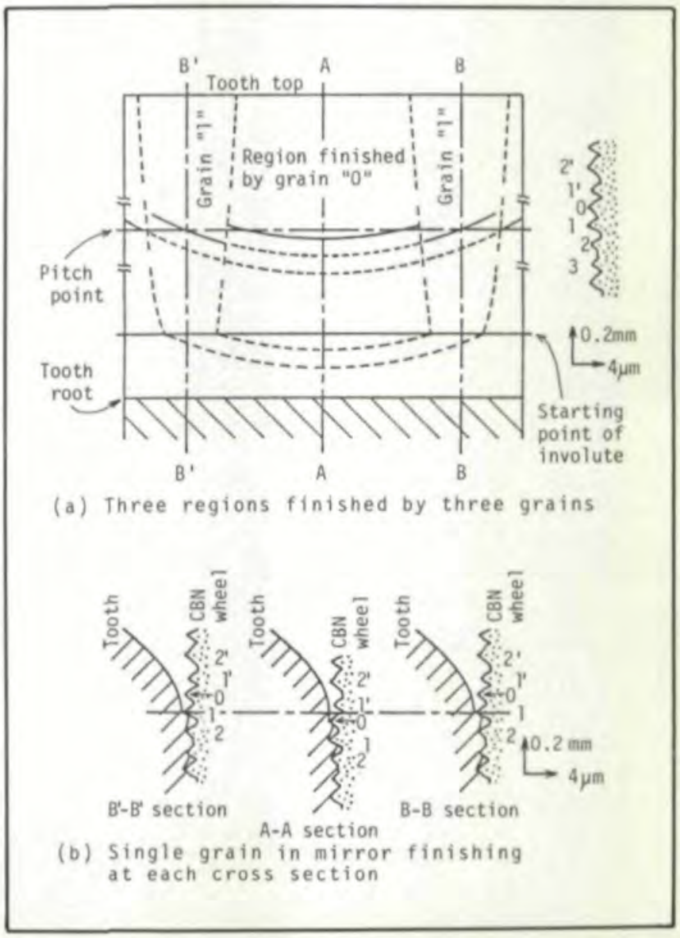

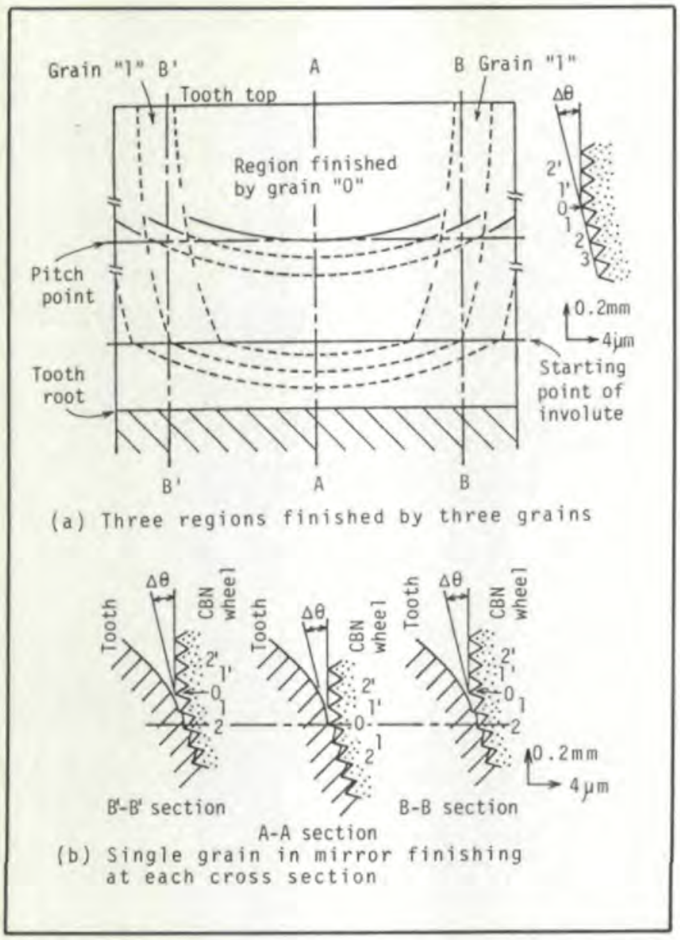

Fig. 7—Mechanism of mirror finishing by wheel with wear

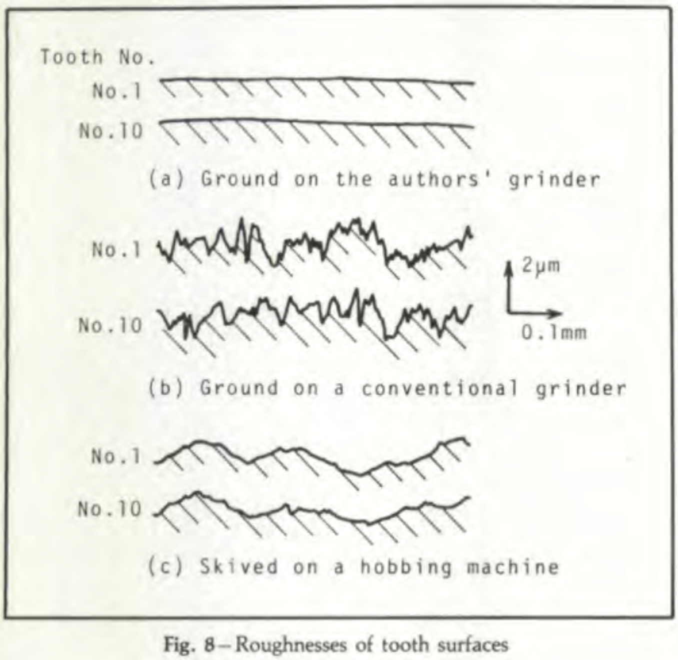

Fig. 8—Roughnesses of tooth surfaces

previously mentioned.

Fig. 11 shows surfaces of two CBN wheels with which mirror finished tooth surfaces were easily obtained at a work rolling speed less than 20 mm/min and a depth of cut less than 30 μm. For clarification purposes, Fig. 12 shows surface roughnesses of teeth finished under grinding conditions outside the best for mirror finishing. When the CBN wheels

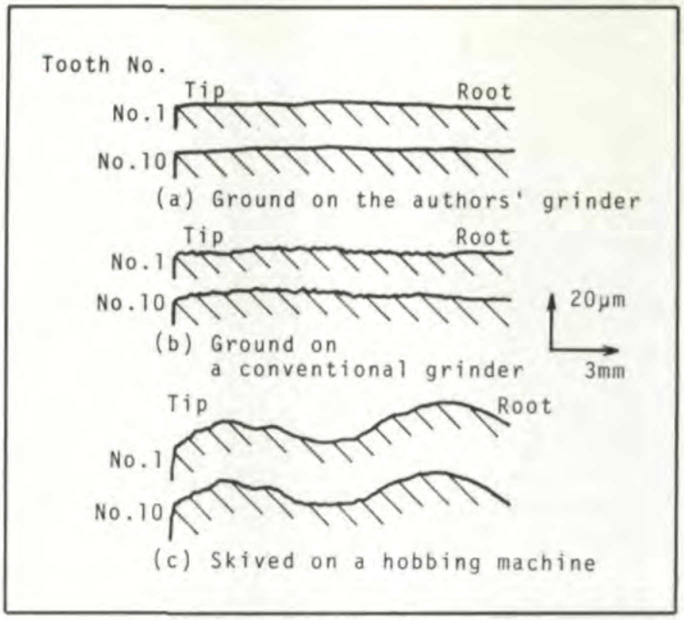

Fig. 9—Tooth profiles of three gears

with grain sizes of #100 and #200 were used, surface roughnesses in the range of 0.2 to 0.4 μm R_{max} were obtained at a work rolling speed of $V_g = 60$ mm/min and a depth of cut $\sigma = 30$ μm. When the CBN wheel with a grain size of #50 was used, mirror finished tooth surfaces were obtained by reducing the work rolling speed to 10 mm/min. However, some waviness was observed at the surfaces, and therefore, the surface quality was not as good as that finished by the wheels with a grain size of #100 or #200.

Increases in the wheel speed are beneficial for obtaining a smoother surface if the vibration of the wheel can be avoided at higher speeds. See Figs. 12(b) and (b′).

Effects of Depth of Cut

As estimated from the mechanism of mirror finishing, tooth surface roughnesses hardly increase when the depth of cut is increased at a constant work-rolling speed. Fig. 13 shows surface roughnesses of teeth finished at a work rolling speed of $V_{2g} = 20$ mm/min. The surface roughness of teeth finished at a depth of cut of 3 μm was about 0.1 μm R_{max} ($\doteq$ 1.0 μ in. Ra). When the depth of cut was increased by a factor of about 30, the surface roughness increased to about 0.5 μm R_{max}.

Effects of Grinding Fluid

Application of grinding fluid is very effective for improving both the surface finish and accuracy of the tooth trace. Fig. 14 shows surface roughnesses and tooth traces of gears finished with and without grinding fluid. In dry grinding, insufficient cleaning of removed chips sticking to the edges of the abrasive grains and insufficient removal of the grinding heat bring about reduction in the surface quality of teeth ground. Thermal expansion of gear teeth is greater at and near the center of the face width. Due to this effect, the tooth traces become appreciably concave when the depth of cut and/or the work rolling speed exceed a certain limit.

Application of a small amount of grinding fluid improves surface roughness appreciably as seen in Fig. 14(b). In order

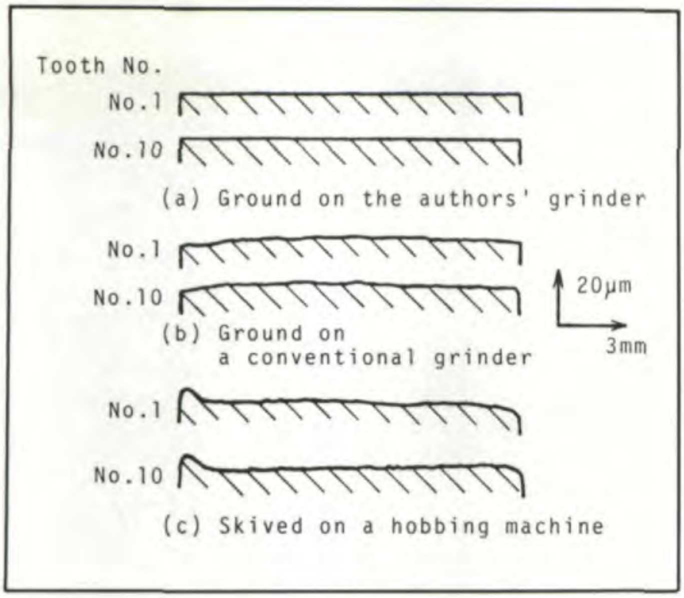

Fig. 10—Tooth traces of three gears

to prevent the thermal effect which brings about concave tooth traces, a larger amount of grinding fluid must be applied to the tooth being ground.

Wear and Grinding Ratio of CBN Wheels

Using the trial gear grinder, the wear and the grinding ratio (volume of removed metal/worn volume of grinding wheel) of CBN wheels were investigated under different grinding conditions.

Effects of Grinding Fluid

Fig. 15 shows an example of the grinding ratios obtained in finishing of hardened gears with a hardness of about 800 HV using a resinoid CBN wheel with a grain size of #200. Wheel and work speeds were 1130 m/min and 20 mm/min, respectively. Effects of grinding fluid upon the grinding ratio were very small under these moderate grinding conditions. In some cases, grinding fluid can prevent abnormal wear under severe grinding conditions.

Effects of Wheel Speed and Bonding Material

The effects of the CBN wheel speed upon the wear of the wheel were comparatively small. Fig. 16 shows changes in the worn volume when the resin bonded (resinoid) and metal bonded wheels were used at speeds of 1800 and 3600 rpm. It should be noted that the worn volume of the CBN wheel with metal bonded grains was appreciably smaller than that of the resin bonded wheel. Increase in the wheel speed caused an increase in the wear of the wheel. This is contrary to the general expectation based on the results obtained in the high speed grinding with Alundum wheels.[8]

Fig. 17 shows grinding ratios obtained when grinding hardened gears using the resin bonded and metal bonded wheels with the same grain size (#100). Grinding conditions (V_g = 60 mm/min, σ = 30 μm) were comparatively severe, and therefore, grinding fluid was applied at a flow rate of 6 L/min. When the resinoid wheel was replaced by the metal bonded wheel, the grinding ratio increased by a factor of about 6. However, this replacement of wheels brought about

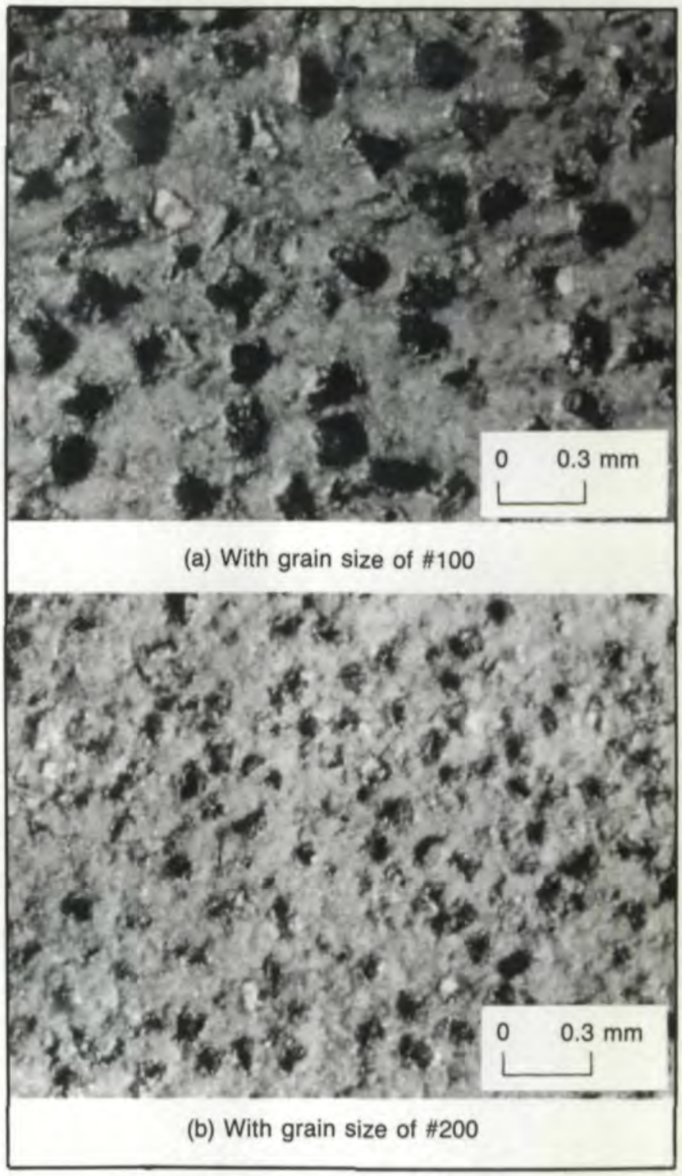

Fig. 11—Surfaces of resinoid CBN wheel

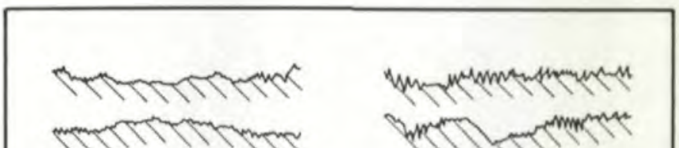

Fig. 12—Effects of grain size and wheel speed upon roughnesses

(continued on page 22)


THE NEW GLEASON
G-MAXX™
BEVEL GEAR GENERATOR
GLEASON

THE FIRST TRULY UNIVERSAL BEVEL GEAR GENERATOR EVER MADE

First ever CNC bevel gear generator.

First with two *and* three axis geometries.

First with such superior machine accuracy.

The new Gleason G-MAXX™ 2010 bevel gear generator can give you strong, quiet, high quality gears more productively, more cost efficiently than any other generator ever made.

First In Flexibility

You get three axis geometry for quick, accurate, continuous hobbing. You get a completed gear and pinion in one chucking.

You also get two axis geometry for cutting, grinding and hard finishing by the intermittent face mill process.

The new Gleason G-MAXX generator is designed to either stand alone or function in an automated systems manufacturing environment.

No other generator ever made gives you such choices.

First In Electronics

You program and store your machine settings with Computerized Numeric Control. CNC controls the speed and position for cutter, cradle, workspindle, and sliding base to drastically reduce your set-up time. You can handle smaller, more diverse runs more productively.

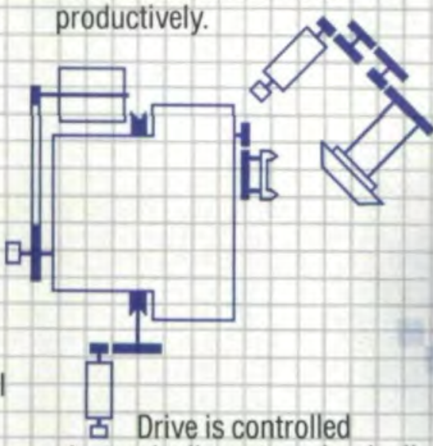

Drive is controlled electronically, not mechanically. A shorter drive train maximizes the accuracy and finish of your gear.

First In Tooling

For continuous hobbing, alternate blade design of our exclusive TRI-AC™ cutter allows for more blade groups per head. You can cut far faster than with conventional cutters. Coated front blade surface reduces tool wear so you can cut far more pieces before sharpening. When you do sharpen, coating stays intact. You get a higher quality finish that requires up to 50% less lapping time.

First In Savings

It all adds up. Prime flexibility, CNC control, high accuracy, fast setup, and high quality gear sets can elevate your productivity to greatly diminish your overall cost per piece. And that's the number one benefit to your bottom line.

Ask For A First Cut

We'll be happy to run a comparative manufacturing cost analysis based on your bevel gear needs. Talk to your Gleason representative or call us direct. 716-473-1000. Or write Gleason Works, 1000 University Avenue, Rochester NY 14692 USA. See for yourself all the cost efficient solutions the new Gleason G-MAXX 2010 Generator can bring to you.

GLEASON

G-MAXX and TRI-AC are Trademarks of Gleason Works

CIRCLE A-7 ON READER REPLY CARD

an increase in surface roughnesses. Of course, mirror finished tooth surfaces with a roughness of about 0.2 μm R_{max} can be achieved using the metal bonded CBN wheel when the grinding conditions are properly selected.

Effects of Work Speed

The grinding ratio changes with the work rolling speed at the same wheel speed. Fig. 18 shows grinding ratios obtained under different work rolling speeds using a resinoid CBN wheel with a grain size of #200. The grinding ratio increased with the work rolling speed up to a certain limit (about 800 at V_g = 60 mm/min and σ = 30 μm), and thereafter, decreased due to the effect of abnormal wear. The abnormal wear is caused by the detachment of effective grains with strong cutting ability. This detachment is due to excessive force acting at the cutting edges of the grains.

Effects of Work Hardness

It is generally believed that the ground surfaces become a little rougher when the hardness of work materials is made lower. However, mirror finishing of low hardness gears was achieved when the authors' grinder was used. For example, Fig. 19 shows surface roughnesses of a gear with a hardness of 290 HB. Mirror finished surfaces with a roughness of about 0.1 μm were obtained at a comparatively large depth of cut (30 μm) but a low work-rolling speed of 6 mm/min.

Note that the wear of CBN wheels becomes appreciably larger in the grinding of low hardness steel gears. Fig. 20 shows grinding ratios obtained in grinding of a high hardness gear with 800 HV and a lower hardness gear with 290 HB. In grinding the lower hardness gear, the lower grinding ratios were obtained when the work rolling speed was increased from 20 to 60 mm/min. This result is contrary to the one obtained when grinding high hardness gears.

The appreciably lower grinding ratios obtained in the grinding of low hardness steel may be ascribed to the higher plastic deformability which brings about a difficulty in production of grinding chips.

Discussion

Errors Caused by Wear of Grinding Wheel

Wear of CBN wheels is very small under normal grinding conditions, and its effect is negligible in grinding one test gear.

Comparison with Alundum Wheel

In order to compare their cutting ability, two Alundum wheels with much the same grain sizes as those of the CBN wheels were used on the trial gear grinder. Fig. 21 shows changes in the tooth profiles and tooth traces of a hardened gear of up to 150 teeth, ground by an Alundum wheel without re-dressing. The tooth trace error (concavity) was clearly observed after grinding 150 teeth when the ground surface began to burn. In the case of the CBN wheel, a sufficient grinding ability had been retained under the same grinding conditions and no traces of burning were seen on the tooth surfaces even after grinding 150 teeth or more. Accuracies of the gear ground by the CBN wheel were better than those of the gear ground by the Alundum wheel as shown in Fig. 22.

Changes in Hardness Due to Grinding

It is generally accepted that CBN wheels can grind cooler than Alundum wheels and hardly bring about tempering effects at and below ground surfaces. However, it is better to use a grinding fluid when the grinding conditions are comparatively severe. Fig. 23 shows changes in hardnesses of four gears ground with and without grinding fluid. In the case of fully hardened gears, an appreciable decrease in hardness was

Fig. 13—Effects of depth of cut upon surface roughness

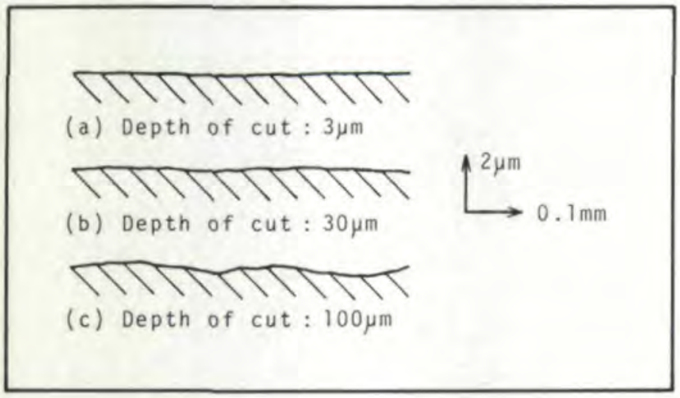

Fig. 14—Surface roughnesses and tooth traces (Effect of grinding fluid)

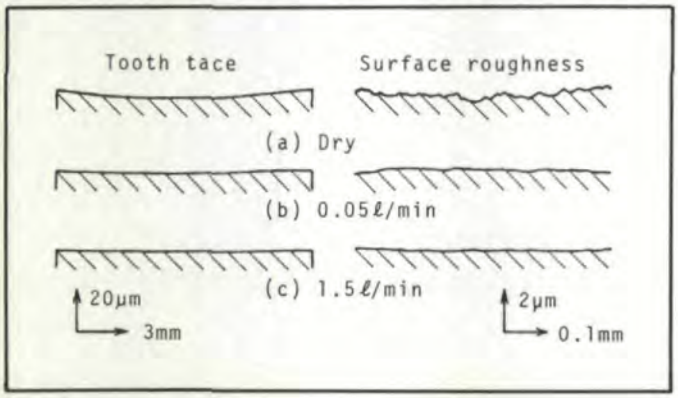

Fig. 15—Grinding ratio in dry and wet grinding

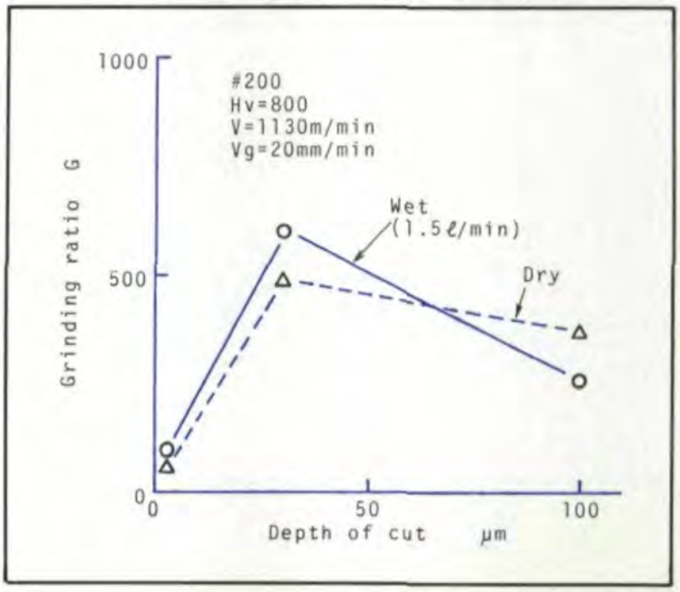

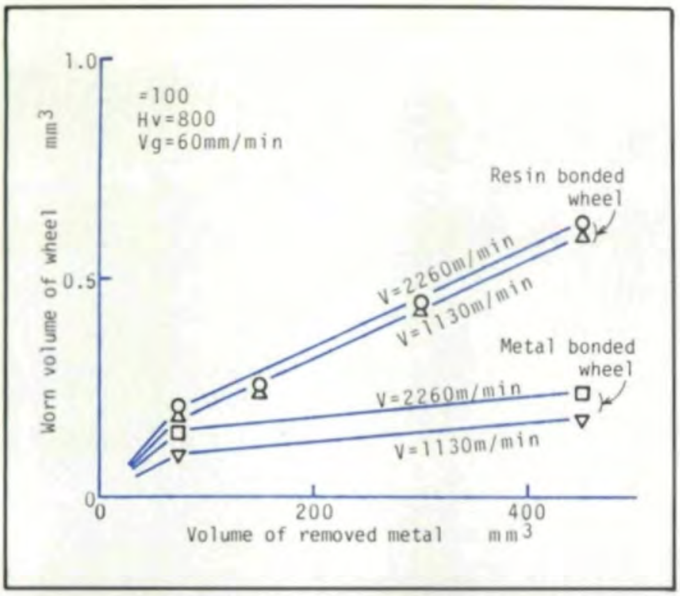

Fig. 16 – Effects of grain bonding material upon wheel wear

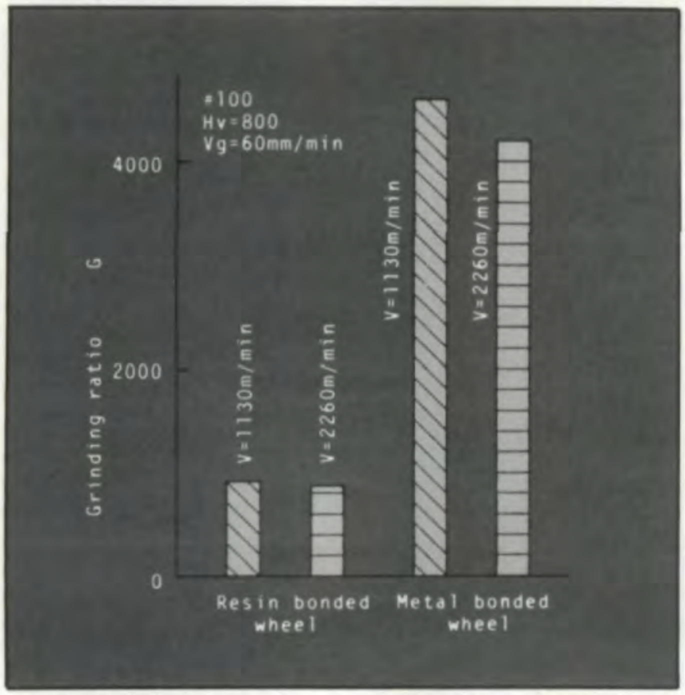

Fig. 17 – Effects of grain bonding material upon grinding ratio

observed in dry grinding, while an increase in hardness was observed in the case of a lower hardness gear with 290 HB. In wet grinding with a non-soluble grinding fluid flooded at a rate of 1.5 L/min, no decrease in the hardness was observed in the fully hardened gear.

Application to Other Grinders

The results shown in this article can be applied effectively to improve a shaving-cutter grinder because its grinding process is almost the same as that in the trial gear grinder.

Mirror finishing of circular-arc tooth-trace cylindrical gears will be possible when a cup-type grinding wheel with an effective surface at and near the edge is used. Note, in this case that the face milling cutters[9] cannot be used for rough and semi-finishing of gears.

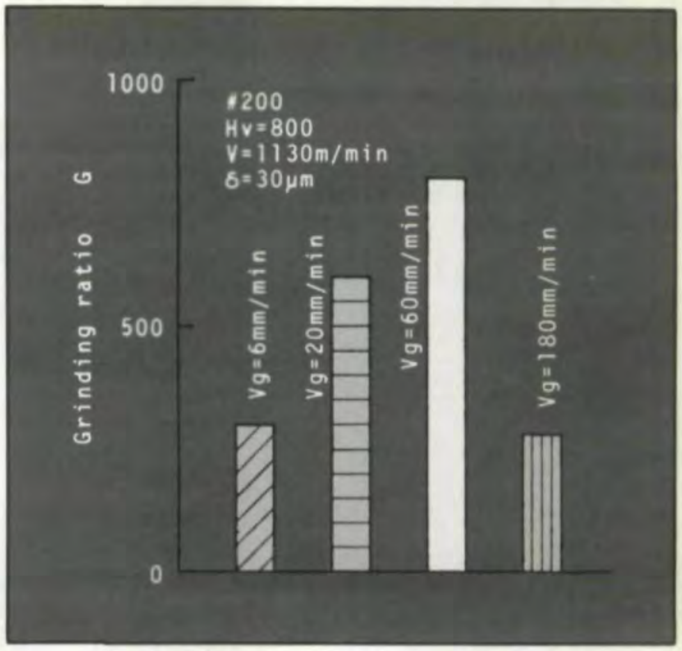

Fig. 18 – Effects of work speed upon grinding ratio

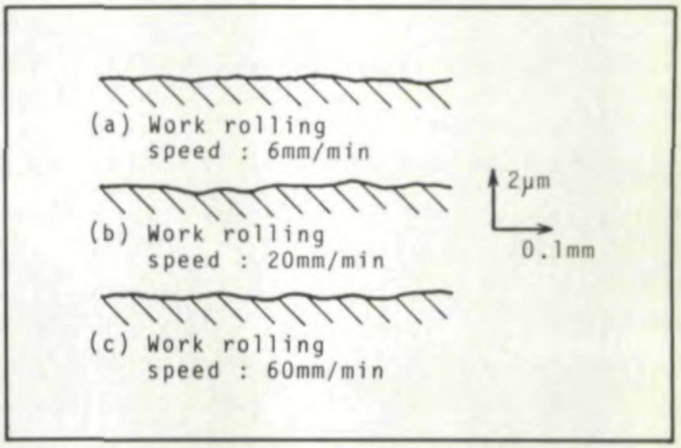

Fig. 19 – Surface roughnesses of lower hardness gear

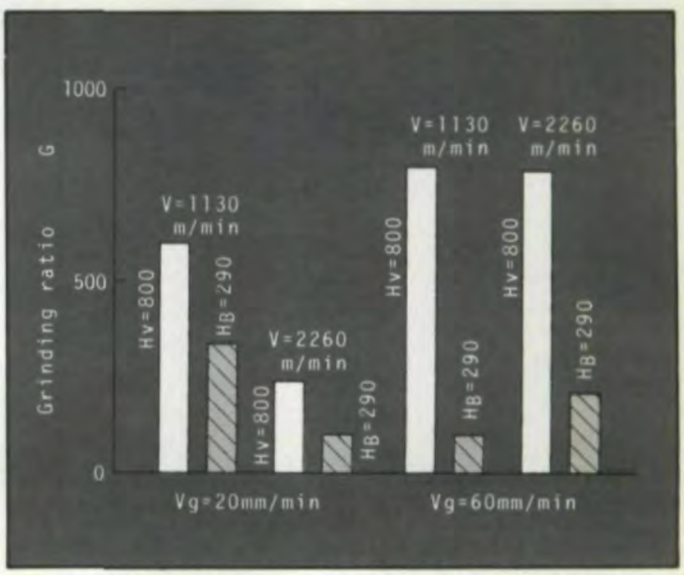

Fig. 20 – Effects of gear hardness upon grinding ratio

(continued on page 26)

Vertical Hob Sharpener

For straight gash hobs up to 6-in. dia. by 6-in. long. Indexing accuracy for "Class A" tolerances without using index plates.

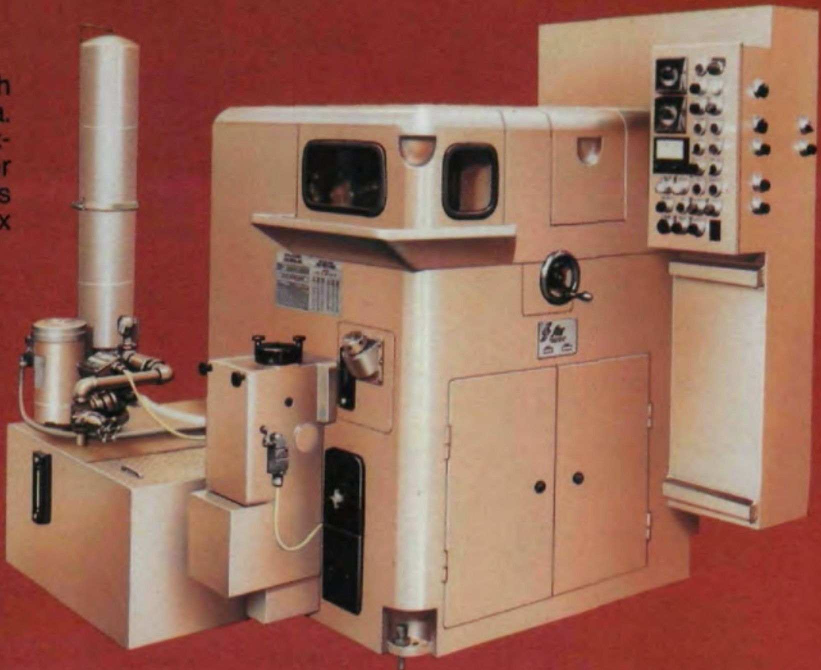

Star SHARPENING

...the economical and
for your tool sharpen

CNC Drill & Reamer Sharpener

This five axis machine allows users to automatically resharpen tools to their original manufacturing specifications.

These domestically manufactured machines have fully programmable automatic grinding cycles and user needs are fully accommodated in their design. We provide on-site engineering service and training to our customers.

CNC Hob Sharpener

For straight gash hobs up to 10-in. dia. by 12-in. long. Indexing accuracy for "Class AA" tolerances without using change gears or index plates.

MACHINES

ractical solution
ng requirements.

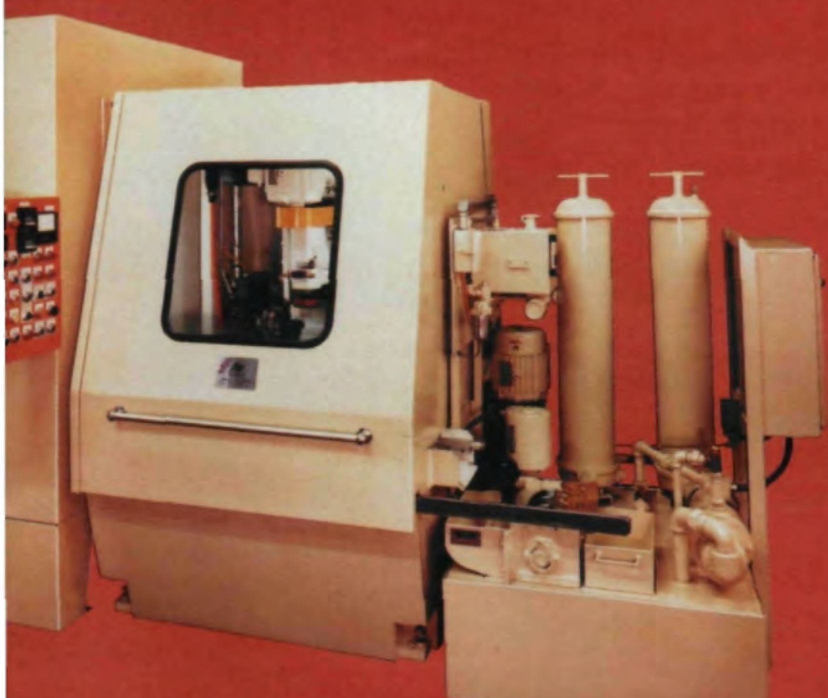

Shaper Cutter Sharpener

For both spur type and right- or left-hand helical type shaper cutters. Fully programmable, totally automatic cycles.

STARCUT SUPPLIED PRODUCTS AND SERVICES

Star Machine Tools
Standard and CNC Hob Sharpeners
Shaper Cutter Sharpeners
CNC Drill and Reamer Sharpeners

Star Cutting Tools
Hobs
Form-Relieved Cutters
Gun Drills
Gun Reamers
Keyseat Cutters

Gold Star Coatings

Lorenz
Shaper Cutters

Hurth Machine Tools
Automatic Spline Shaft Milling Machines
CNC Gear Shaving Machines
CNC Gear Rolling Machines
Gear Testing Machines
Shaving Cutter Grinding Machines
CNC Gear Tooth Chamfering Machines
Gear Deburring Machines
CNC Hard Gear Finishing Machines

Hoefler
CNC Inspection Equipment for Gears and Gear Cutting Tools

TiN Coating Systems
Complete Turnkey Applications

PLANRING USA, INC.
Planning & Engineering
Flexible Machining Systems

Stieber
Precision Clamping Tools

Please contact us for further information on any or all of these sharpening machines and other StarCut supplied products and services.

Since 1927
Star
STARCUT SALES, INC.
23461 Industrial Park Drive
Farmington Hills, MI 48024
313/474-8200 Telex 230-411

CIRCLE A-5 ON READER REPLY CARD

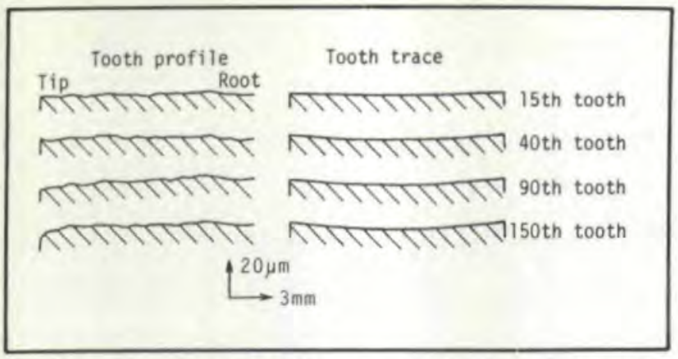

Fig. 21 – Tooth profiles and tooth traces with Alundum wheel V – 1240 m/min, V_g – 60 m m/min, σ – 30 μm

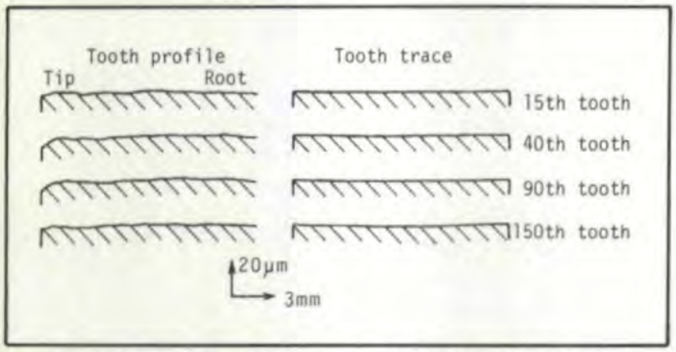

Fig. 22 – Tooth profiles and tooth traces with CBN wheel V – 1130 m/min, V_g – 60 mm/min, σ – 30 μm

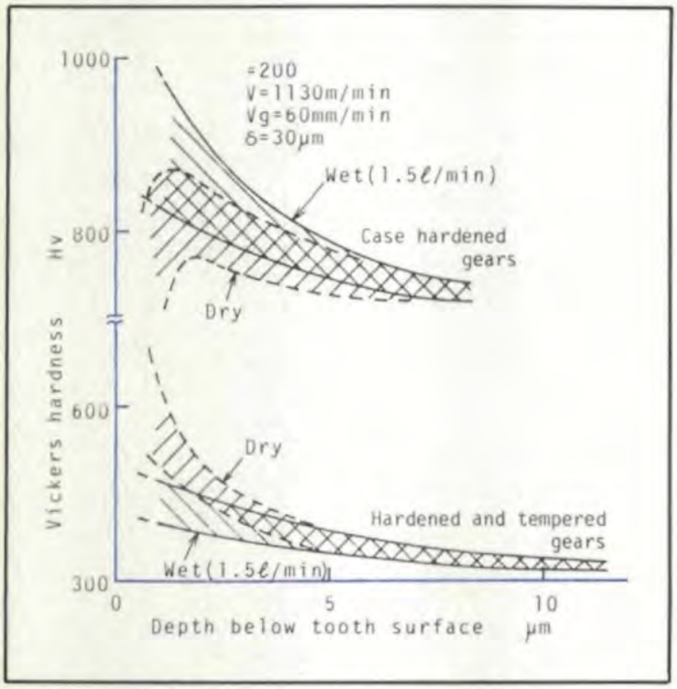

Fig. 23 – Changes in hardness of ground gear

Production Rate in Mirror Finishing of Gears

As described in the mechanism of mirror finishing and the experimental results, mirror finishing of tooth surfaces can be achieved at a lower work rolling speed less than 100 mm/min. However, a comparatively large depth of cut (30-50 μm) is allowable in the mirror finishing when sufficient grinding fluid is applied to the grinding region. Notice that mirror finished tooth surfaces can be obtained without the use of the spark-out grinding process. This saves much time in the final grinding process. Rough grinding is possible, leaving a finishing stock of 10-30 μm, and then mirror finishing can be done by a single pass of the wheel. For example, mirror finishing of the test gears with 25 teeth could be achieved within 20-30 minutes when the trial gear grinder was used. Production rates in mirror finishing of tooth surfaces will be improved in the future. At the present time, it may be estimated that mirror finishing of tooth surfaces may be performed at a production rate acceptable in practice.

Conclusions

Using a gear grinder designed and made by the authors, the following results were obtained:

(1) In contrast to the general expectation that CBN wheels produce rougher surfaces than conventional Alundum wheels, very smooth mirror-like surfaces have been obtained using a CBN wheel (Fig. 1).

(2) The mechanism of mirror finishing with CBN wheels has been clarified and supported by experiments.

(3) Mirror finished tooth surfaces with a roughness of about 0.1 μm R_{max} ($\doteq$ 1.0 μ in. R_a) are easily obtained using CBN wheels with grain sizes of #100 and #200.

(4) Mirror finishing of low hardness gears is possible, but the grinding ratio in the mirror finishing becomes appreciably smaller than that in the grinding of fully hardnened gears.

(5) Grinding ratios obtained using a metal-bonded CBN wheel are appreciably greater than those obtained with a resin-bonded CBN wheel,but the tooth surface quality with the metal-bonded wheel is a little lower under the same grinding conditions.

(6) It is better to use grinding fluid for improving the surface finish and also for avoiding the reduction in hardness at and near the ground surface of fully hardened gears.

References

1. FIELD, J.E., "The Properties of Diamond", Academic Press, London, 1979, p. 396.
2. ISHIBASHI, A., and NAKAE, M., "Wear of HSS Hob Ground by Boron-Nitride Wheel and Accuracy and Surface Durability of Gears Hobbed", *Bull. Japan Soc. Pre. Eng.*, Vol. 15, No. 2, June 1981, p. 137-138.
3. KÖNIG, et al., "Teilwälzschleifen von Einsatzgehärteten Zylinderräderen mit CBN-Doppelkegelscheiben", ant-antriebstechnik, Bd. 20, Nr. 7-8, 1981, s. 314-317.
4. DAIMON, M., et al., "Performance of CBN Wheel; 4th Report", Preprint of Japan Soc. Pre. Eng., March 1983, p. 51-54, (in Japanese).
5. For example, more than a hundred papers are shown in the following paper: Yokokawa, K., "CBN Wheels and Future of Grinder", *Tool Engineer*, Vol. 26, No. 12, Dec. 1982, p. 95-101, (in Japanese).
6. YOKOKAWA, K., "Performance of CBN Wheel; 14th Report," Preprint of Japan Soc. Pre. Eng., Oct. 1983, p. 533-534, (in Japanese).
7. KISHI, K., et al., "Wear Characteristics of Resin Bonded CBN Wheel", Preprint of Japan Soc. Pre. Eng., Oct. 1983, p. 527-528, (in Japanese).

(continued on page 48)

A Logical Procedure To Determine Initial Gear Size

by
Abraham I. Tucker, P.E.
Gear Engineering
San Diego, California

Abstract

A logical procedure is described for determining the minimum size gear set required to transmit a given load for a given operating life. Variations of this procedure are applied to different gear arrangements. These include speed reducers, speed increasers, star and planet reducers, and star and planet increasers. A logic flow diagram is included for computer application.

Introduction

When a gear set is to be designed for a new application, the minimum size gears with the required capacity are desired. These gears must be capable of meeting the power, speed, ratio, life, and reliability requirements.

The intent of this article is to present a logical and orderly sequence of steps to determine this size. The term "size" refers to the diameters and face widths. On multi-stage gear units this procedure would be applicable to one stage at a time.

For the sake of simplicity, it is assumed here that the gear set is steel and that the hardness of the meshing gears are alike and are given in the Rockwell C scale. Gears of differing hardness or gears on the BHN scale can also use this type of procedure. AGMA 218.01[1] provides equations to determine the allowable stresses.

AUTHOR:

The late **ABRAHAM I. TUCKER** *was a consulting engineer specializing in gear-related engineering problems. He had experience in the design and development of high speed, high performance gear assemblies, hydrodynamic bearings for gearing and turbomachinery and lubrication systems for high speed machinery.*

A graduate of New York University, Mr. Tucker was the author of several technical papers. He was a Registered Professional Engineer and a member of ASME and Tau Beta Pi and Pi Tau Sigma honor societies.

Basic Equation

The basic equation for this procedure is derived from the classical Hertz equation for the surface compressive stress on two curved surfaces. It has been rearranged to produce a solution for a minimum pinion diameter.[2] For an external gear set it is

$$d \geqslant \left[\frac{0.7\ Tp\ E\ (mg + 1)\ (\cos HA)^2\ Kd}{Sc^2\ R\ mg\ \sin PAn\ \cos PAn\ mp}\right]^{1/3} \qquad (1)$$

For an internal gear set the term (mg −1) would be used in place of (mg +1).

Pinion Torque

The torque on the pinion determines its required size and, consequently, the size of the entire gear train. By definition, a pinion is the smallest member in a gear train. In a speed reducer it would be the driver. In a speed increaser it would be the driven member. In an epicycle train it may be either the sun or the planet (or star), depending on the ratio. Fig. 1 illustrates these differences. This will be considered in the equations which follow.

One of the major factors which determines the gear size is the transmitted torque through the pinion, Tp. Input data required to determine this torque are as follows:

1. Input speed, ni, rpm
2. Desired output speed, no, rpm
3. Horsepower, P
4. Number of equal power paths, K
5. Type of gear arrangement.

If the gear set is simple speed reducer, either single mesh or multiple countershaft, then:

$$Tp_1 = \frac{63025\ P}{ni\ K} \tag{2}$$

$$mg_1 = ni/no \tag{3}$$

If it is a simple speed increaser, then:

$$Tp_2 = \frac{63025\ P}{no\ K} \tag{4}$$

$$mg_2 = no/ni \tag{5}$$

For a speed reducer which has a star arrangement, where the input is to the sun and output is from the ring, and where $3 \leq Mg \leq 10$, the sun is the pinion. This will be designated as STAR 1. See Fig. 1. Then:

$$Mg = \frac{ni}{no} \tag{6}$$

$$mg_3 = \frac{Mg - 1}{2} \tag{7}$$

$$Tp_1 = \frac{63025\ P}{ni\ K} \tag{2}$$

When the star set reducer ratio is $1.2 \leq Mg < 3$, each star is a pinion. This will be designated as STAR 2. See Fig. 1. Then:

$$mg_4 = \frac{2}{Mg - 1} \tag{8}$$

$$Tp_3 = \frac{63025\ P}{ni\ mg\ K} \tag{9}$$

If the star set is a speed increaser and the input is to the ring, the output to the sun and the carrier would be fixed. Similar reasoning may be applied to determine which item is the pinion, its transmitted torque, and the diameter ratio of sun to star, mg.

For a planet type speed reducer where the ring is fixed, the input is to the sun and output is through the carrier. If the speed ratio is $4 \leq Mg \leq 11$, the sun is the pinion. This will be designated as PLANET 1. See Fig. 1. Then:

$$mg_5 = \frac{Mg - 2}{2} \tag{10}$$

$$Tp_1 = \frac{63025\ P}{ni\ K} \tag{2}$$

If the planet set speed ratio is $2.2 < Mg < 4$, the planets are the pinions. This will be designated as PLANET 2. See Fig. 1. Then:

$$mg_6 = \frac{2}{Mg - 2} \tag{11}$$

$$Tp_3 = \frac{63025\ P}{ni\ mg\ K} \tag{12}$$

If the planetary set is a speed increaser, the input is to the carrier, output is to the sun, and the ring gear is fixed.

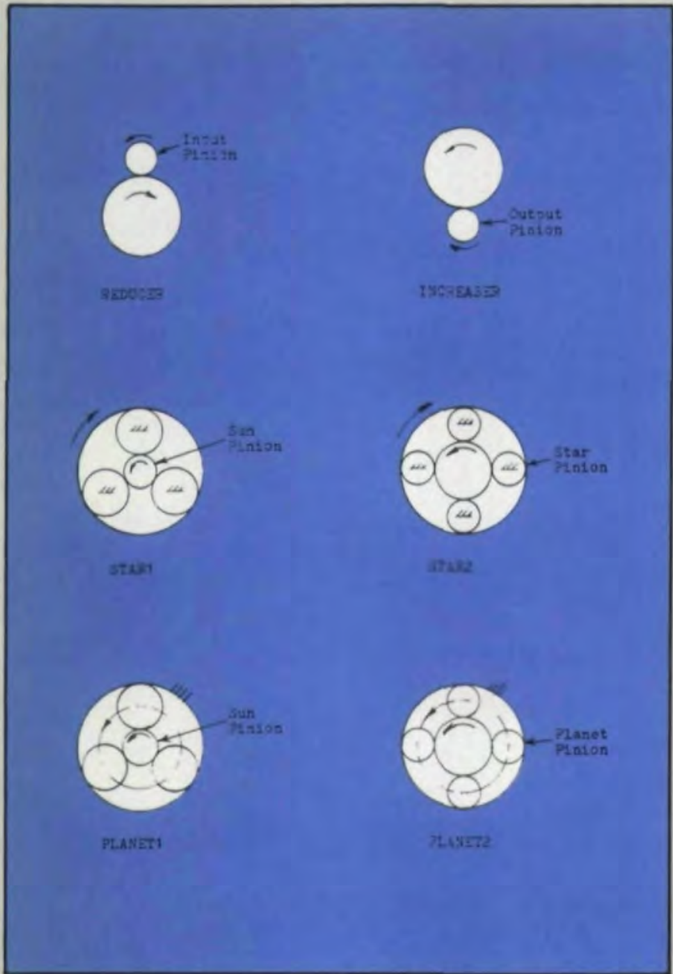

Fig. 1 – Some common gear arrangements showing the location of the pinion in the train.

Depending on the ratio, similar logic may be applied to determine which member is the pinion, its transmitted torque, and the diameter ratio of the sun and planet, mg.

Allowable Contact Stress

The allowable contact stress, Sc, for a given fatigue life in hours, Lh, is the next factor which determines the required gear size. To determine this allowable stress the input data needed are

1. Desired life in number of hours, Lh.
2. Material hardness, Rockwell C scale, HRC.

Allowable contact stresses at 10^7 cycles, Sac, are specified in AGMA 218.01, Table 5.[1] An equation to determine the conservative end of these allowable stresses would be

$$\mathrm{Sac} = 3333.33\ \mathrm{HRC} \tag{13}$$

The life in hours must next be converted to number of contact cycles, N.

$$\mathrm{N} = \mathrm{Lh}\ 60\ \mathrm{ni}\ \mathrm{K} \text{ for speed reducers} \tag{14}$$

$$\mathrm{N} = \mathrm{Lh}\ 60\ \mathrm{no} \text{ for speed increasers} \tag{15}$$

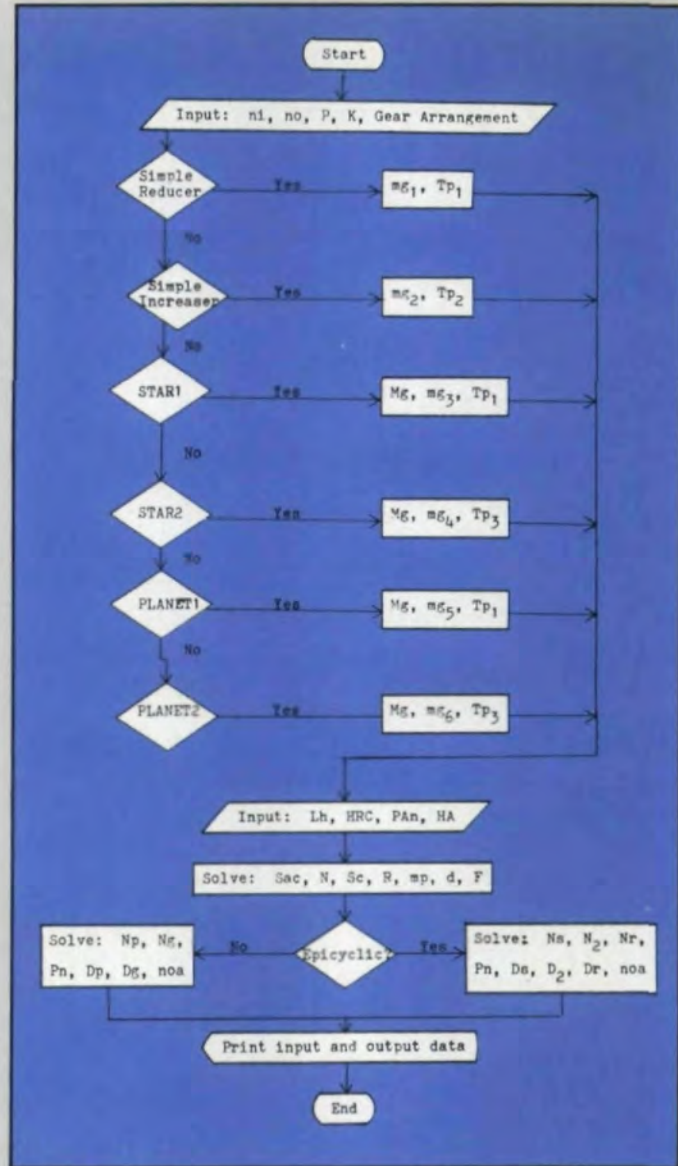

Fig. 2 – Flow Diagram.

The maximum allowable stress from 0 to 10^4 cycles is constant. Therefore, if $N < 10^4$, then let $N = 10^4$.

Between 10^4 and 10^7 cycles, the allowable contact stress, Sc, to meet the fatigue life per AGMA 218.01 is

$$\mathrm{Sc} = \mathrm{Sac}\ \frac{2.466}{\mathrm{Lc}^{.056}} \tag{16}$$

Above 10^7 cycles, the allowable contact stress to meet the fatigue life is

$$\mathrm{Sc} = \mathrm{Sac}\ \frac{1.4488}{\mathrm{Lc}^{.023}} \tag{17}$$

Minimum Pinion Size

To determine the minimum pinion size, some additional input data are required.

A. For new designs, a reasonable ratio of F/d is desired. The face width should be short enough to minimize the effects of lead errors and shaft deflections. It should not be too short, or the required diameter would be too large.

Nomenclature

Dg = Gear pitch diameter
Dp = Pinion pitch diameter
Dr = Ring gear pitch diameter
Ds = Sun gear pitch diameter
D_2 = Star or planet pitch diameter
d = Minimum required pinion pitch diameter
E = Young's modulus
F = Face width
HA = Helix angle
HRC = Hardness, Rockwell C
IP = Integer part
K = Number of equal power paths
Kd = Derating factor
Lc = Life in number of cycles
Lh = Life in hours
Mg = Reduction ratio, epicyclic gear train
mg = Ratio of gear/pinion diameters
mp = Profile contact ratio
N = Number of life cycles
Ng = Number of teeth in gear
Np = Number of teeth in pinion
Nr = Number of teeth in ring gear
Ns = Number of teeth in sun
N_2 = Number of teeth in star or planet
Nri = Initial estimate of number of teeth in ring gear
ni = Input speed, rpm
no = Output speed, desired, rpm
noa = Output speed, actual, rpm
P = Horsepower
PAn = Pressure angle, normal
Pn = Diametral pitch, normal
PLANET 1 = A planetary set where $4 \leq Mg \leq 11$
PLANET 2 = A planetary set where $2.2 \leq Mg < 4$
R = Ratio, F/d
Sc = Allowable contact stress at the desired fatigue life, psi
Sac = Allowable contact stress at 10^7 cycles, psi
STAR 1 = A star gear set where $3 \leq Mg \leq 10$
STAR 2 = A star gear set where $1.2 \leq Mg < 3$
Tp = Pinion torque, lb. in.

A reasonable initial F/d ratio would be

$$R = \frac{mg}{mg + 1} \qquad (18)$$

B. The normal pressure angle, PAn, and the helix angle, HA, must be provided as initial input data. They influence the surface curvature and the resultant surface compressive stress. A reasonable initial estimate for the profile contact ratio would be

$$mp = 2.54 - .04\ PAn \qquad (19)$$

C. In the basic equation, mp is applicable only to helical gears. Therefore, for spur gears, HA = 0 and mp = 1.

D. An initial estimate for the total derating factor, Kd, is required. This estimate could be set to an initial value of 2. A more precise value could be determined after the size and pitch line velocity are known. The basic equation could then be reiterated.

This completes the initial input data. The minimum required gear size can now be determined using the basic equation:

$$d = \left[\frac{.7\ Tp\ 29.5\ 10^6\ (mg + 1)(\cos HA)^2\ Kd}{Sc^2\ R\ mg\ \sin PAn\ \cos PAn\ mp}\right]^{1/3} \qquad (1)$$

and

$$F = d\ R \qquad (20)$$

Numbers of Teeth and Diametral Pitch

When the minimum pinion diameter is determined, an integer number of teeth and a diametral pitch must be chosen. For simple meshes a practical number of pinion teeth, gear teeth, and diametral pitch may be determined by the following equations:

$$Np = \left[IP\ 17\ \frac{mg + 2}{mg} \cos HA + 1\right] \qquad (21)$$

(Note: The above equation is an empirical determination which would normally provide teeth stronger in bending than in surface compression.)

$$Ng = IP\left[(Np\ mg) + .5\right] \qquad (22)$$

$$Pn = IP\left[\frac{Np}{d \cos HA}\right] \qquad (23)$$

Final pitch and gear pitch diameters would be

$$Dp = \frac{Np}{Pn \cos HA} \qquad (24)$$

$$Dg = \frac{Ng}{Pn \cos HA} \qquad (25)$$

For star or planet trains, an empirical equation to determine a reasonable number of pinion teeth would be

$$Np = IP\left[17 \frac{mg + 1}{mg} \cos HA + 1\right] \qquad (26)$$

Then:

$$Pn = IP\left[\frac{Np}{d \cos HA}\right] \qquad (23)$$

To determine numbers of teeth in the other gears in star or planet sets, the following procedures are required:

1. For a "STAR 1" or "PLANET 1" reducer the sun gear is the pinion. Therefore:

$$Ns = Np \tag{27}$$

2. For a "STAR 2" or "PLANET 2" reducer the stars or planets are the pinions. Therefore:

$$Ns = IP\left[(Np\ mg) + 1\right] \tag{28}$$

3. For all star reducers, an initial estimate for number of ring gear teeth would be

$$Nri = Ns\ Mg \tag{29}$$

4. For all planet reducers an initial estimate for number of ring gear teeth would be

$$Nri = Ns(Mg - 1) \tag{30}$$

The sum of the teeth in the sun and ring must be divisible by the number of stars or planets. The result must be an integer. The following procedure will accomplish this.

$$X = IP\left[\frac{Nri + Ns}{K} + .5\right] \tag{31}$$

$$Nr = K\ X - Ns \tag{32}$$

$$N_2 = \left[IP\ \frac{Nr - Ns}{2}\right] \tag{33}$$

Pitch diameters of the gears in the epicyclic train would then be

$$Ds = \frac{NS}{Pn\ \cos HA} \tag{34}$$

$$D_2 = \frac{N_2}{Pn\ \cos HA} \tag{35}$$

$$Dr = \frac{Nr}{Pn\ \cos HA} \tag{36}$$

With the numbers of teeth now known, actual output speed, noa, and the precise reduction ratio, Mg, may be determined.

The procedures above for determining numbers of teeth and diametral pitch will provide gear sets with pinions slightly larger than the required minimum. This approach is intentionally conservative.

A logic flow diagram of this gear size determination is shown in Fig. 2. It may be used as a guide to program this procedure on a computer.

Conclusion

A complete and logical procedure can be applied to determine the size of a gear set to carry a given load for a given required life. The examples herein show the procedures for applying this logic to several varieties of gear trains. It can be expanded to include many additional types of gear train arrangements, such as epicyclic speed increasers. The steps are in a logical sequence to provide easy programming for a computer or on a calculator. They will prove useful to the design engineer who is given a complete set of requirements or specifications and must then design a suitable gear set starting with a blank piece of paper.

References

1. AGMA 218.01 – AGMA Standard for Rating the Pitting Resistance and Bending Strength of Spur and Helical Involute Gear Teeth. American Gear Manufacturers Association, Arlington, Virginia.
2. TUCKER, A. I., ASME Paper 80-C2/DET-13, The Gear Design Process.

This article was originally printed by the American Society of Mechanical Engineers as Paper No. 84-DET-67

GEAR TECHNOLOGY wishes to thank Mrs. Mona Tucker for permitting us to use this article.

TECHNICAL CALENDAR

November 11-13, 1986
SME Gear Processing and Manufacturing Clinic
Chicago, IL

Call for Papers: The Society of Manufacturing Engineers has issued a call for papers for this meeting. Please submit all papers on or before July 15th. The clinic will also include vendor tabletop exhibits.

For more information, contact Joseph A. Franchini at SME (313) 271-1500, ext. 394.

November 19-21, 1986
Seminar: Gear System Design for Minimum Noise
University of Wisconsin

This course provides an overview of noise control in gear system design and offers practical design information with a minimum of acoustical theory. The course is for engineers who design or specify gears or gear drives.

For additional information contact:
John Leaman at (414) 224-4189.

1987 GEAR MANUFACTURING SYMPOSIUM— CALL FOR PAPERS

The American Gear Manufacturers' Association is issuing a call for papers for its 1987 Gear Manufacturing Symposium to be held April 12-14, 1987, at the Hyatt Regency Hotel, Dearborn, MI. Papers on basic gearing, traditional processes, quality control, materials and emerging technologies will be accepted. Authors are asked to submit abstracts as soon as possible.

For further information contact:
Harry Kidd
American Gear Manufacturers' Association
1500 King Street, Suite 201
Alexandria, VA 22341
Phone: (703) 684-0211.

VIEWPOINT

Letters for this column should be addressed to Letters to the Editor, GEAR TECHNOLOGY, P.O. Box 1426, Elk Grove Village, IL 60007. Letters submitted to this column become the property of GEAR TECHNOLOGY. Names will be withheld upon request; however, no anonymous letters will be published. Opinions expressed by contributors are not necessarily those of the editor or publishing staff.

Dear Editor:

The concept of your book from its first issue has been very important to me. After all of these years, there has always been something new and very important in every issue, so that missing one of your issues would leave a very blank spot in my reference file.

William W. Kern
Stahl Gear & Machine Co.
Philadelphia, PA

We would like to extend our sincere congratulations to you regarding your magazine "Gear Technology".

I was lucky enough to come across a copy while attending the International Machine Tool Show at McCormick Place, Chicago. I had never seen your publication and must say I was very impressed.

We are a gear manufacturing company located in Montreal, Canada. We feel your magazine is very informative and will definitely be most useful in our business and for this reason would like to continue receiving all future editions.

Once again — congratulations and keep up the good work!

Ron Mehra, President
UniGear, Canada

You sure turn out a beautiful magazine. So pretty that I hate to throw it away. In fact have not.

I first got mixed up with gear cutting about 1918. My senior paper at MIT in 1925 was on Gear Inspection. I ran Ohio Gear Cp up until 1965 and have had this operation since 1952.

My father who died in 1931 and who founded Browning Crane in Cleveland was a lover of Leonardo.

Harrison Browning
Arizona Gear &
Manufacturing Co.

Curvic® Coupling Design

Gleason Works
Rochester, New York

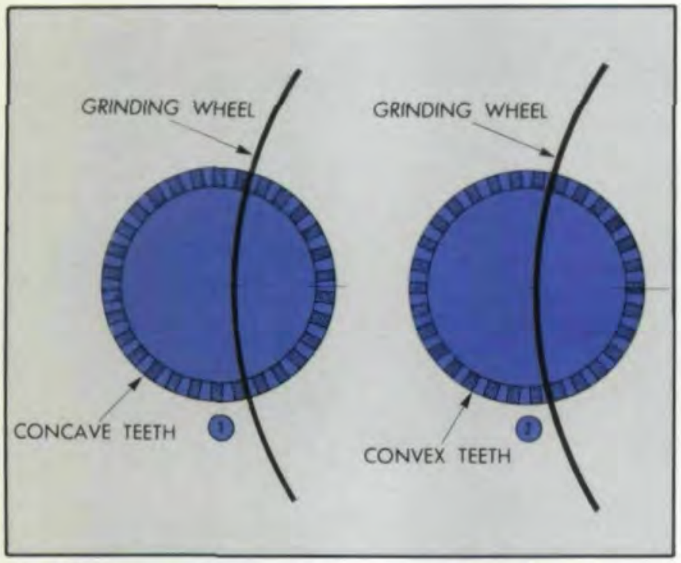

Fig. 1 – Left, a cross-section view taken perpendicular to the axis of a concave Curvic Coupling. Right, the mating convex Curvic Coupling. Note the curved teeth.

Introduction

Curvic Couplings were first introduced in 1942 to meet the need for permanent couplings and releasing couplings (clutches), requiring extreme accuracy and maximum load carrying capacity, together with a fast rate of production. The development of the Curvic Coupling stems directly from the manufacture of Zerol® and spiral bevel gears since it is made on basically similar machines and also uses similar production methods. The Curvic Coupling can therefore lay claim to the same production advantages and high precision associated with bevel gears.

The term "Curvic Couplings" refers to toothed connection members with the teeth spaced circumferentially about the face and with teeth which have a characteristic curved shape when viewed in a place perpendicular to the coupling axis (see Fig. 1.). This curvature exists because the members are machined with a face-mill cutter or a cup-type grinding wheel. One member is made with the outside edge of the cutter or wheel as shown at the left of the figure, and a concave, or an hour glass shaped tooth is produced. The mating member is usually cut or ground with the inside edge, thus producing a convex, or barrel-shaped tooth. The radius of the cutter or the grinding wheel surface is chosen in such a way that the teeth will either mate along the full face width of the tooth or along only a section of the face width, as desired.

The three basic types of Curvic Couplings are (1) the Fixed Curvic Coupling, (2) the Semi-Universal Coupling, and (3) the Releasing Coupling (or clutch). The coupling provides a positive drive along with precision centering and high load carrying capacity.

Fixed Curvic Couplings

The Fixed Curvic Coupling is a precision face spline for joining two members, such as two sections of a shaft, to form a single operating unit.

The fixed Curvic Coupling is used extensively in the construction of built-up turbine and compressor rotors for air-

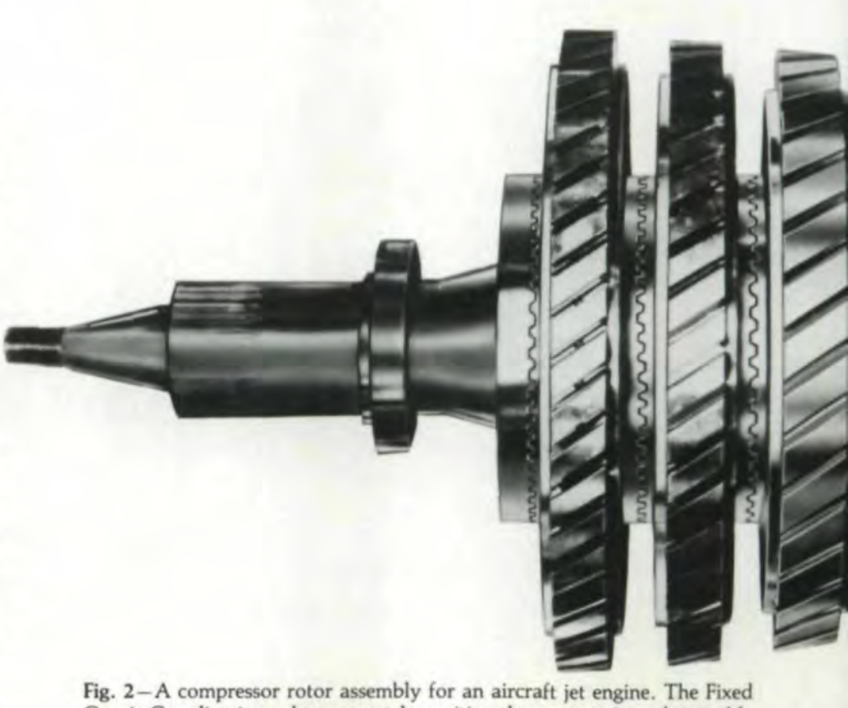

Fig. 2 – A compressor rotor assembly for an aircraft jet engine. The Fixed Curvic Coupling is used to accurately position the separate interchangeable discs.

craft and industrial gas or steam turbine engines as shown in Figs. 2, 3, and 4. Figs. 5 and 6 show a method of joining a turbine impeller or a bevel gear to a shaft. Crankshafts can be made of separate, interchangeable parts by means of a coupling as shown in Fig. 7.

The Fixed Curvic Coupling is also used today by many major machine tool manufacturers for precision indexing mechanisms as illustrated in Figs. 8 and 9.

Semi-Universal Couplings

The Semi-Universal Coupling is also a precision face spline loosely coupled to permit up to 2° misalignment of shafts together with axial freedom. The teeth of one member usually have a curved profile to keep the load localized in the middle of the tooth and to transmit more nearly uniform motion.

Fig. 10 illustrates an application of semi-universal couplings and shows the typical tooth shape.

Releasing Couplings (Clutches)

The Releasing Couplings are designed and made so that the proper tooth contact is maintained while the clutch engages and disengages. In the larger sizes, a helical surface is used to accomplish this. On small clutches, this action is approximated by a special localized tooth bearing. The two members of a shift or overload clutch are usually held in position by spring pressure. By adjusting the amount of pressure, the amount of torque which can be transmitted without disengagement of the clutch can be controlled. Shift clutches are used today in a wide variety of applications including aircraft, automotive, farm equipment and power tools.

The application shown in Fig. 11 can be produced by cutting or grinding, depending on accuracy required.

Fig. 3 – A turbine rotor assembly for a stationary gas turbine. Note the Fixed Curvic Coupling teeth between each disc.

Design Features

The basic geometry of the Curvic Coupling has been given in Fig. 1. The grinding wheel sweeps across the face of the coupling contacting one side of one tooth and the opposite side of another tooth in a single engagement. During one complete revolution of the work, the machining of the Curvic Coupling is completed.

The radius of the grinding wheel, the number of teeth, and the diameter of the Curvic Coupling are all interdependent as shown in Fig. 12.

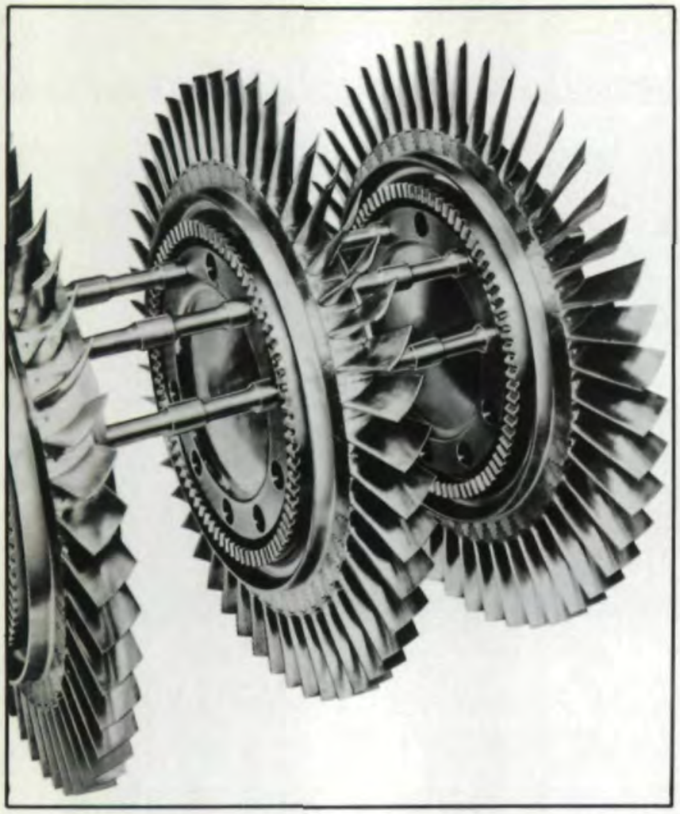

Fig. 4 – A stationary gas turbine rotor showing the through bolts used for clamping the Fixed Curvic Coupling members together.

Fig. 5 – A Fixed Curvic Coupling used in assembling a turbine impeller and shaft.

Fig. 6 – Curvic Couplings are used to enable separate manufacture of bevel gear and long shaft.

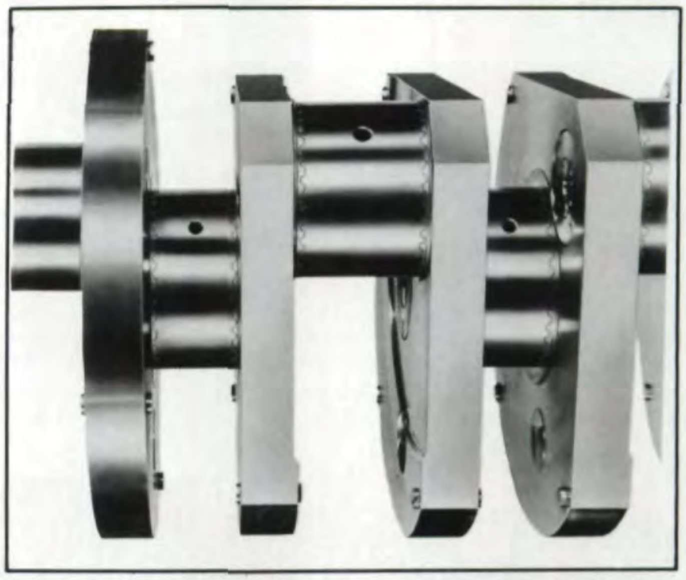

Fig. 7 – A section of a crankshaft showing the Fixed Curvic Coupling. Crankpins, crankwebs and journals were made separately for ease of manufacture and handling.

The basic relationship is as follows:

n_x = number of half pitches included between two engagements of grinding wheel.

N = *number of teeth in Curvic Coupling.*

r = radius of grinding wheel.

A = mean radius of Curvic Coupling.

then $\beta = \frac{90° \times n_x}{N}$

and $r = A \tan \beta$.

The radius of the grinding wheel can be changed by changing n_x as well as by changing N and A. The diameter of the grinding wheels used varies between nominal values of 6"

Single flank testing goes digital.

FIND OUT WHAT THE NOISE IS ALL ABOUT.

When it comes to pinpointing the causes of gear vibration and noise, it's no secret that single flank measurement gives you the kind of comprehensive data you simply can't get with other forms of measurement. Reliable information about *transmission error* is what you need to predict noise potential of a gear set in operation, as well as to reduce process errors and the costly scrap and rework that go with it.

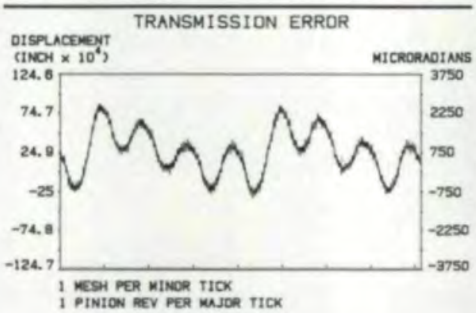

But the analog (graphic) results of single flank testers can be time consuming to analyze—even for an experienced operator. So single flank testing hasn't always been practical for production environments.

Until now.

Gleason gives single flank testing "brains."

With Gleason's 579 G-AGE™ Automatic Data Analysis System, ADAS (compatible with any G-AGE Single Flank Tester), test results are generated digitally and graphically to greatly reduce data interpretation time. Featuring the most sophisticated single flank software available today—a Gleason exclusive—this intelligent system rapidly and accurately:

1. Quantifies single tooth-to-tooth composite error, combined pitch variation, combined accumulated pitch variation, single flank composite error and other gear tooth variations.
2. Reveals the noise potential of gear sets.

And with our system's frequency spectrum analysis, the harmonics and side bands of tooth mesh frequency can be observed to let you establish acceptable peak amplitudes for various harmonics. That means you can be sure of a gear's noise potential before it's assembled.

GLEASON AUTOMATED GEAR EVALUATION

	TOLERANCE	MEAS. ERROR	PERCENT OF TOL.
TOT. TRANS. ERROR	+.0060	+.00520	+++++
MAX T-T TRANS. ERROR	+.0007	+.00050	++++
AVG T-T TRANS. ERROR	+.0002	+.00020	REJECT
# OF BURRS OVER TOL	+3.0000	+0.00000	
MAX EFFECTIVE PROF VAR	+.0003	+.00010	++++
AVG EFFECTIVE PROF VAR	+.0002	+.00010	+++
COMB. ACC. PITCH VAR	+.0050	+.00500	REJECT
COMB. MAX PITCH VAR	+.0007	+.00050	++++
COMB. MAX SPACING VAR	+.0015	+.00030	++

(RESULTS IN IN)

Let our brain help your brains be more productive. Call Gleason's Sales Department today and arrange an in-depth, no-obligation consultation about our new 579 G-AGE ADAS.

Call this number today:
(716) 473-1000

Gleason

The Gleason Works, 1000 University Avenue, Rochester, N.Y. 14692

CIRCLE A-14 ON READER REPLY CARD

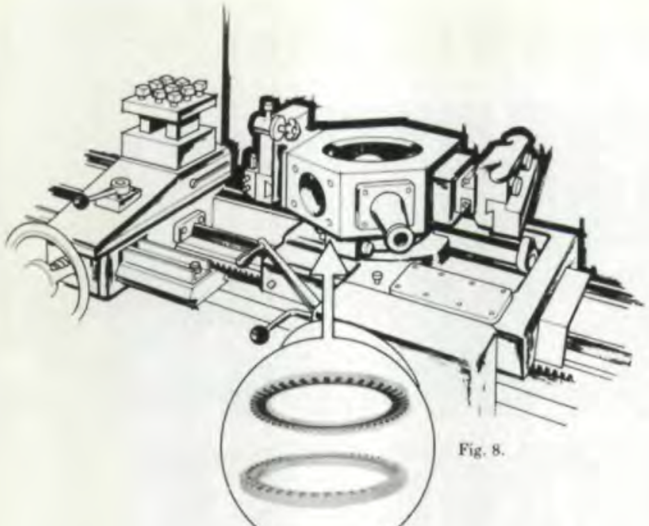

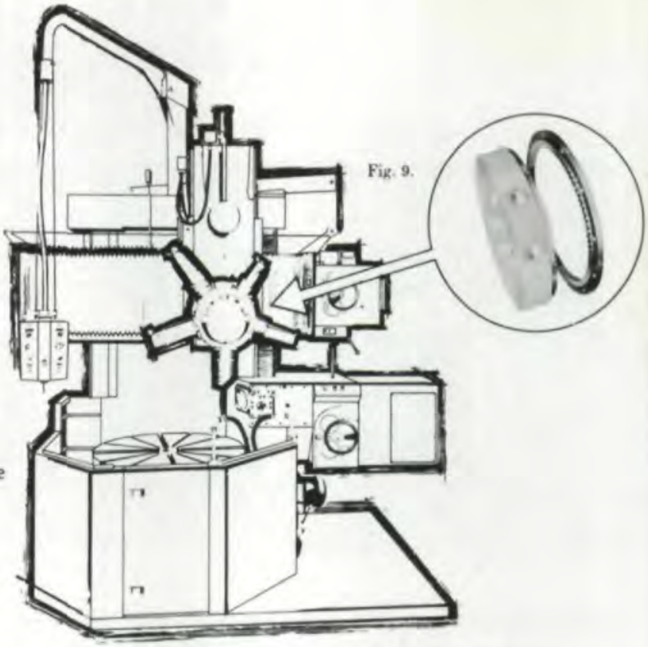

Fig. 8 and 9—The precision accuracy of Fixed Curvic Couplings permits the precise indexing and repeatability required on this horizontal turret lathe (Fig. 8) and vertical turret lathe (Fig. 9).

and 21". The maximum Curvic Coupling diameter produced is 50" and the smallest diameter is 0.375".

Curvic Coupling teeth can be produced with a wide range of pressure angles to suit the application.

A view of ground Fixed Curvic Coupling teeth at the outside diameter is shown in Fig. 13. The chamfer on the top of the teeth is automatically ground as the tooth slot is being ground. The chamfer permits a larger fillet radius to be used, thus strengthening the teeth. Also shown is the characteristic gable bottom which eliminates any possibility of forming a stress-raising step in the root of the tooth. Fig. 14 shows the tooth configuration of a typical Curvic Coupling.

As can be seen in Figs. 1 and 12, the space between two adjacent Curvic teeth is ground at two different locations on the wheel to obtain the proper taper of the tooth toward the coupling center. The grinding wheel then must be wide enough to cover at least half of the tooth space width at the outside diameter and still be narrow enough to pass through the space at the inside.

To do this, the inside diameter of the coupling must be equal to, or greater than, 75% of the outside diameter.

Another design feature of Fixed Curvic Couplings permits localization of the tooth contact area. The tooth contact for most applications should be centrally located and the length of contact should be approximately 50% of the face width when checked with the mating control coupling under light pressure. The type of application and method of bolting determine the tooth bearing length which should be used. Under pressure of the bolting load the tooth bearing area will increase, thus insuring a uniform distribution of contact over the entire tooth surface.

Because the grinding wheel sweeps across the face of the coupling, it is usually necessary that the blank design contain no projections beyond the root line of the teeth. For proper clearance, the nearest projection should be at least $^1/_{32}$" below the root line.

In designing a Fixed Curvic Coupling it is essential to consider the method of bolting or clamping the two members. The tension in the bolt or bolts must be sufficient to keep the coupling teeth in full engagement under all conditions of operation. Furthermore, the bolts must have clearance throughout their entire length so that centering is accomplished only by the Fixed Curvic Coupling teeth.

In selecting the required coupling size, three items determine the load which the coupling teeth will carry. The teeth must (1) be strong enough so they will not shear, (2) have sufficient surface area to prevent pitting, galling, and fretting corrosion, and (3) be supported by adequate material to withstand tension across the root of the tooth space.

The shear strength is dependent upon the cross-sectional area of all the teeth. Since there is no backlash in a Fixed Curvic Coupling, the teeth are in intimate contact so that half of the metal is ordinarily removed in both members, regardless of the number of teeth or their depth. With this condition, the torque load is carried over a shear area approximately half as large as in a one-piece hollow shaft.

The allowable surface loading will depend on the contact area of the coupling teeth. Standard tooth proportions are used to maintain a constant area for a given coupling diameter regardless of the number of teeth. This area is sufficient to carry a load corresponding to the safe load in shear, and the proportions are varied only in special cases.

The third factor affecting the load carrying ability of the coupling is related to the bolt tension. Tension in the bolt

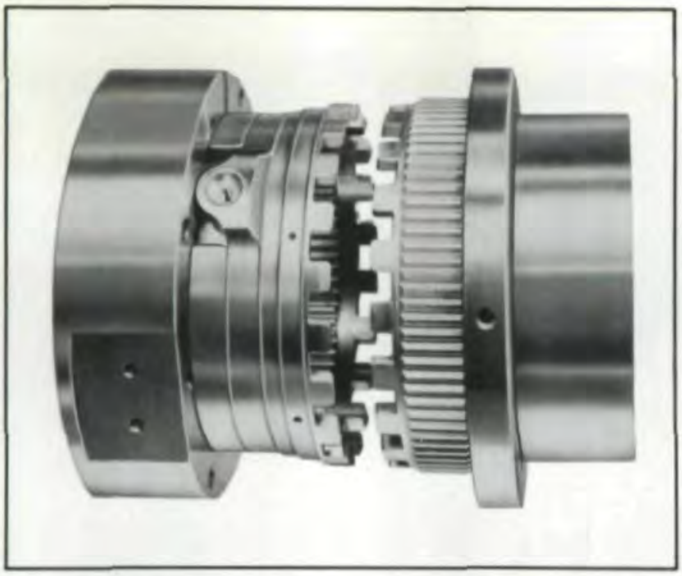

Fig. 10 – A Curvic Coupling of the semi-universal type is employed at both ends of this intermediate drive shaft.

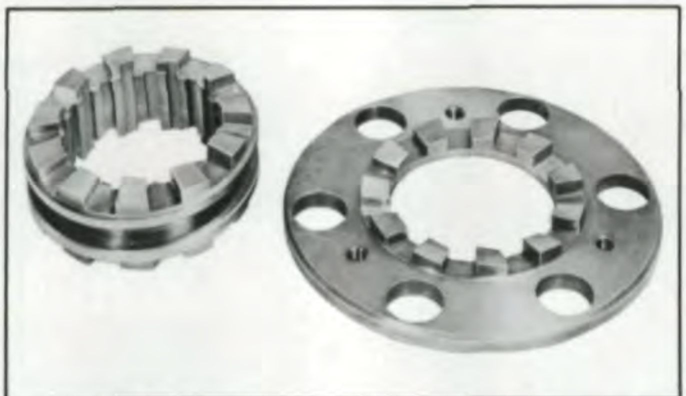

Fig. 11 – A shift clutch for a truck application. The tops of the teeth have generated helical surfaces.

forces the coupling members together causing a wedging effect between the mating teeth. This wedging effect creates a tensile stress in the blank under the tooth space. An increased amount of backing material will decrease this stress within limits.

Design Procedure

After considering the type of Curvic Coupling required to meet the needs of a given application, it is possible to determine the approximate size which is necessary to transmit a specified load.

For initial size determination on Fixed Curvic Couplings either Graph 1 or the following formula can be used:

$$D = \sqrt[3]{\frac{T}{1310}} \quad \text{where } D = \text{coupling diameter (inches)}, \; T = \text{torque (lb-inches)}$$

This assumes that the face length is .125 times the coupling diameter or .875", whichever is smaller, and a material with an ultimate strength of 150,000 P.S.I. is employed. Graph 2 applies to Semi-Universal Curvic Couplings and Graph 3 covers shift and overload clutches which engage or disengage under load. For a shift clutch which is engaged or

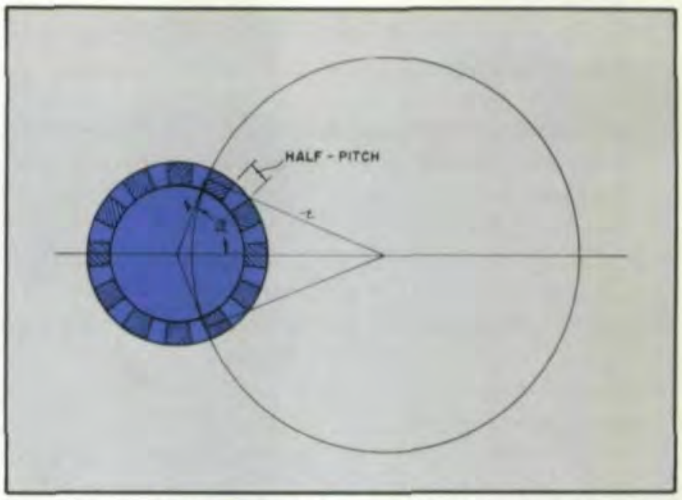

Fig. 12 – Diagram illustrating the basic geometry of the Curvic Coupling.

disengaged only while standing still, use the Graph 1. Graphs 2 and 3 are based on the use of case-hardening steel at 60 Rockwell "C".

The maximum torque value during operation should be used in the above determination. If, however, there is a peak starting torque or other peak overload torque which occurs very infrequently during the life of the unit and does not exceed 5 seconds duration at any one time, this peak value should be divided in half and compared with the maximum operating torque. The higher of these two values should be used to determine coupling size.

Curvic Coupling Design

Having chosen the initial size of the Curvic coupling, it is necessary to determine the number of teeth and the face width. Pressure angle and whole depth will be considered in later sections. When using standard tooth proportions, the surface contact area of the Curvic teeth will remain constant for a given coupling diameter, regardless of the number of teeth. Also, the shear area remains substantially constant for a given coupling diameter, regardless of the number of teeth.

Couplings are usually designed with a diametral pitch ranging from 3 to 8. Graph 4 shows a recommended range for diametral pitch in relation to outside diameter. This curve is intended only as a guide, and the designer may depart from it if special requirements exist. Diametral pitch is taken at the outside diameter and, therefore, the number of teeth equals the diametral pitch multiplied by the outside diameter of the coupling.

The face width of the Curvic coupling is the radial distance between the outside and inside radii of the coupling. It is almost directly proportional to the stress when the outside diameter is held constant. Often, the configuration of the assembly or weight considerations will dictate the face width to be used. The face width is generally .125 of the outside diameter of the coupling in order to produce the Curvic coupling with proper tooth taper.

Curvic Design

The initial Curvic Coupling dimensions which have been chosen in the preceding section should now be checked using the stress formulas for this particular type of coupling.

It is first necessary, however, to list the standard tooth proportions for Fixed Curvic Couplings. Fig. 15 shows a cross-section view of the teeth at the outside diameter and is the standard form for a Fixed Curvic Layout. It shows the symbols used for the various tooth dimensions. Standard depth proportions are recommended for all heavily loaded applications. The 70% of standard tooth proportions are usually satisfactory where less surface contact area is acceptable for the lighter loads.

Fig. 13 – Fixed Curvic Coupling teeth viewed at the outside diameter. Note the gable bottom.

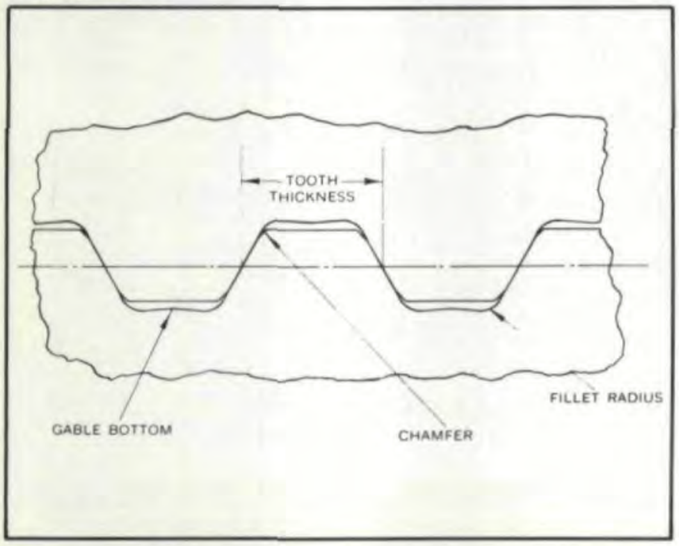

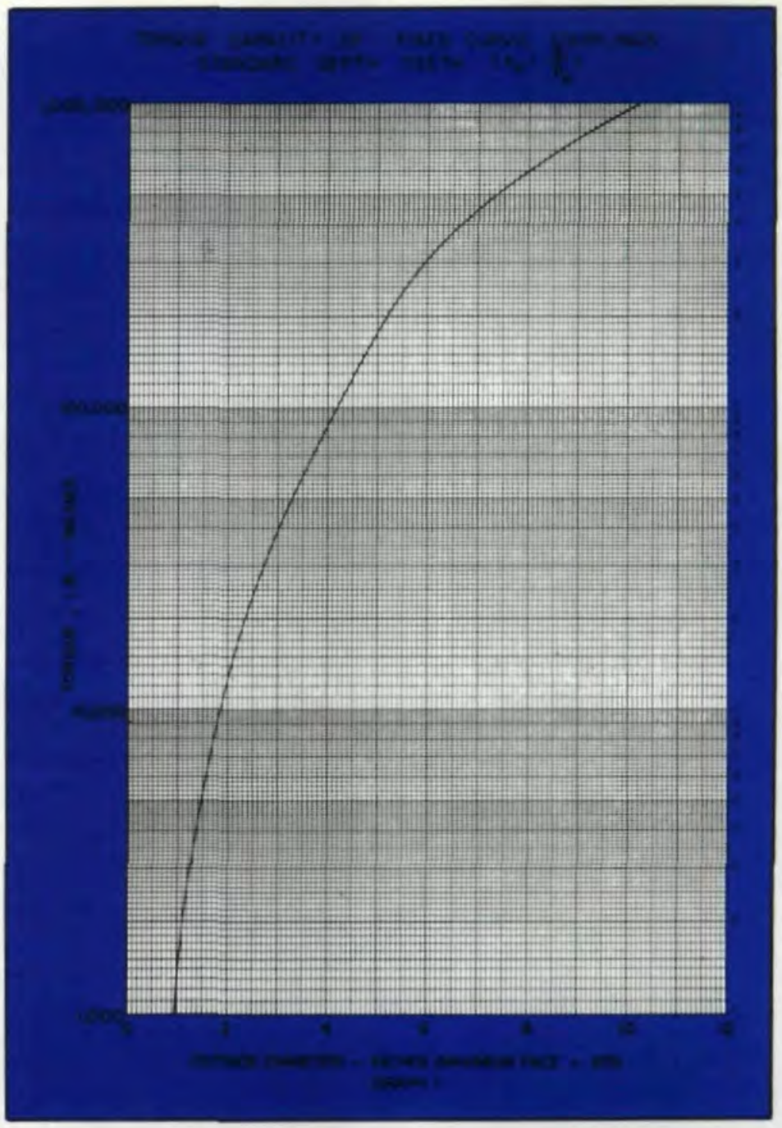

Fig. 14 – The tooth configuration of the Fixed Curvic Coupling is clearly shown on this marine radar part.

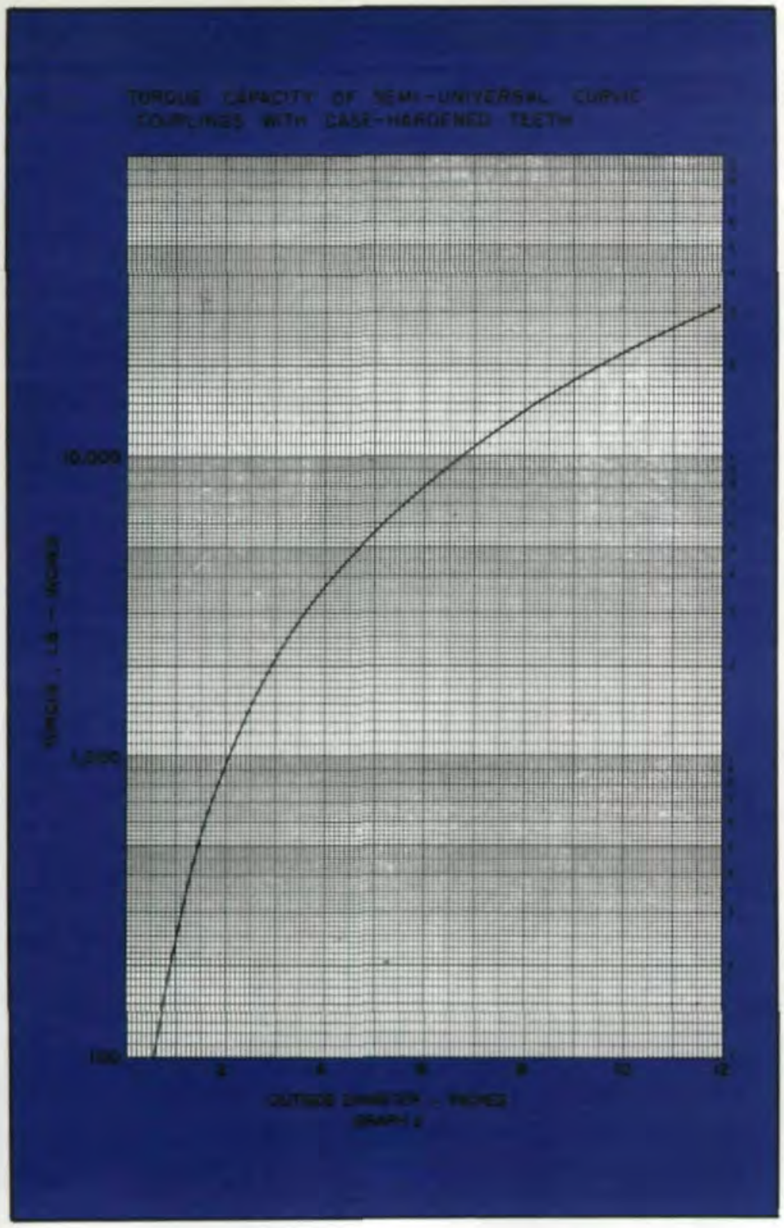

	Standard Tooth Proportions	*Alternate Tooth Proportions*
P_d	N/D	N/D
h_t	$\frac{.800}{P_d}$	$\frac{.616}{P_d}$
c	$\frac{.100}{P_d}$	$\frac{.070}{P_d}$
c_t	$\frac{.090}{P_d}$	$\frac{.063}{P_d}$

The final values should be rounded to the next higher even thousandth.

P_d=diametral pitch at the outside diameter.

$a = \frac{h_t - c}{2}$

$b = h_t - a$

D=coupling outside diameter

c =clearance

c_t=chamfer height

h_t=whole depth

a =addendum

b =dedendum

A pressure angle of 30° has been found to be most practical for most Fixed Curvic Couplings and is the standard. This pressure angle is the best compromise between a low pressure angle, with its corresponding light separating force, and a high pressure angle with its greater strength. Also, the axial and radial runout of the Curvic coupling can be held more accurately at higher pressure angles, such as 30°, since the tooth spacing accuracy is constant for all pressure angles, and the axial component of a given spacing error decreases as pressure angle increases.

If special design conditions require it, the pressure angle for a Fixed Curvic Coupling can be as low as 10° or as high as 40°. The strength formulas given are applied to pressure angles between 20° and 40°. For lower pressure angles, increase the calculated stress up to 25%.

For pressure angles 20° and lower, the amount of clearance should be doubled.

The fillet radius, the tooth thickness and the height of the gable bottom (see Figs. 13 and 15) are calculated on the worksheets for machine settings.

A calculation for shear stress and for surface stress should

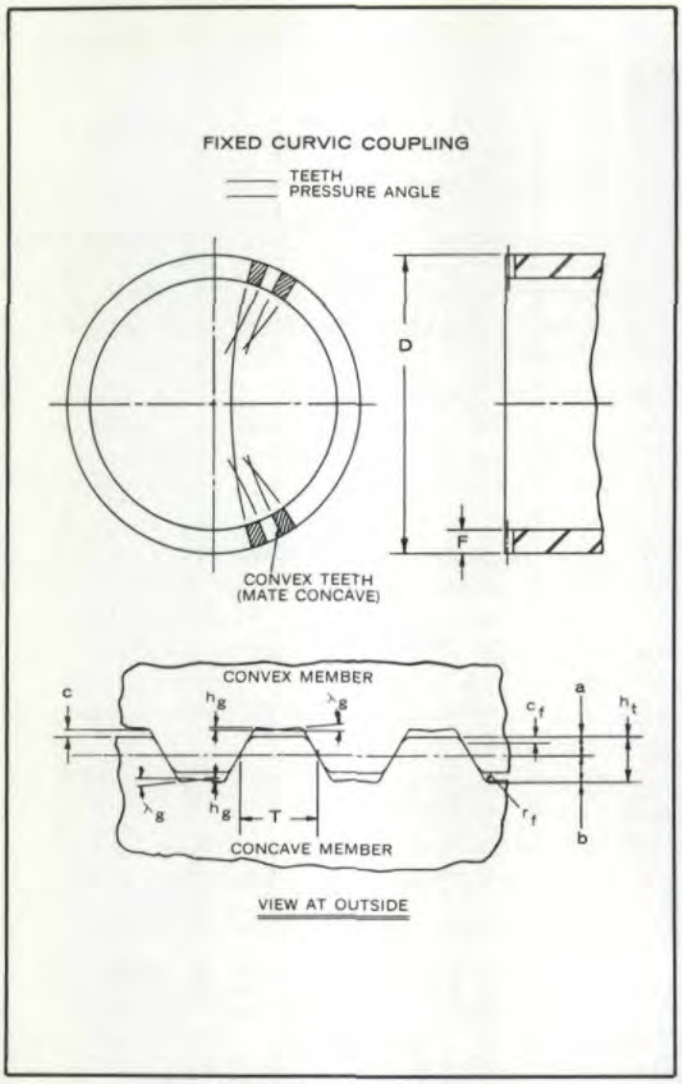

Fig. 15—Fixed Curvic Coupling.

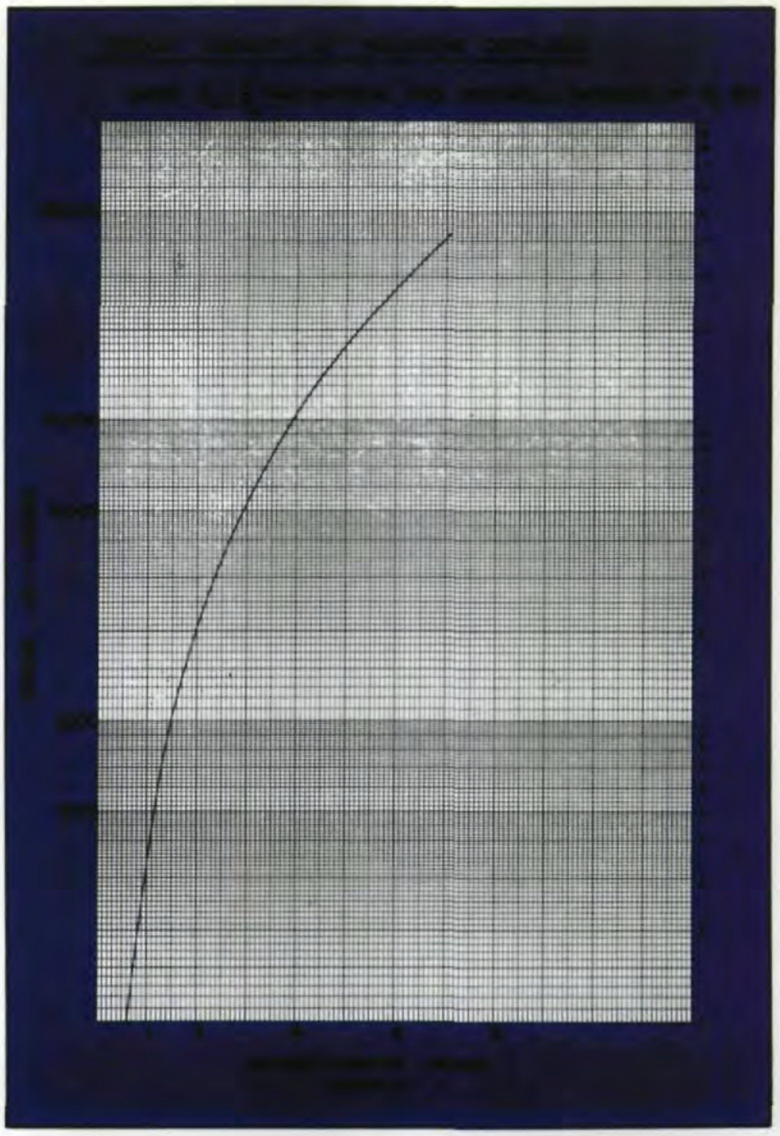

be made according to the following formulas:

$$\text{Shear stress } s_s = \frac{T}{\pi A^2 F}$$

$$\text{Surface stress } s_c = \frac{T}{AFN\ h_o}$$

where T = torque, lbs. inches

A = mean radius of coupling, inches $= \frac{D-F}{2}$

F = face-width, inches

N = number of teeth

h_o = contact depth, inches $= (h_t - c - 2c_t)$

The recommended allowable limit for shear stress is 15,000 psi. when there is combined torsion and bending. The recommended allowable limit for shear stress is 30,000 psi. when there is pure torsion and no bending. The recommended allowable limit for surface stress is 40,000 psi. for all applications. These limits are suitable for continuous operation. Higher stresses may be permissible for very short periods which occur only infrequently during the life of the unit. Continuous operation at higher stresses is likely to result in tooth breakage or surface distress on the Curvic teeth.

The allowable limits listed above are based on the use of steel with an ultimate tensile strength of 150,00 psi. minimum at operating temperatures. For steel with a lower ultimate strength and for other materials such as aluminum, titanium, and various heat-resistant alloys, the allowable limits should be altered in direct proportions to the ultimate strength values at operating temperature.

A pair of Fixed Curvic Couplings must be tightly clamped together in assembly so that the teeth are in actual contact under all conditions of operation. This clamping action is usually provided by a single through bolt or multiple bolts. However, other means such as a special clamp can be used provided the above condition is met. It is important that the clamping arrangement and clamping force be carefully chosen. The bolt or bolts should have clearance throughout their entire length so that centering is accomplished only by the Fixed Curvic Coupling teeth.

The clamping force should be at least one and one-half to two times the sum of *all* the separating forces acting on the Curvic coupling teeth. *These separating forces usually include*

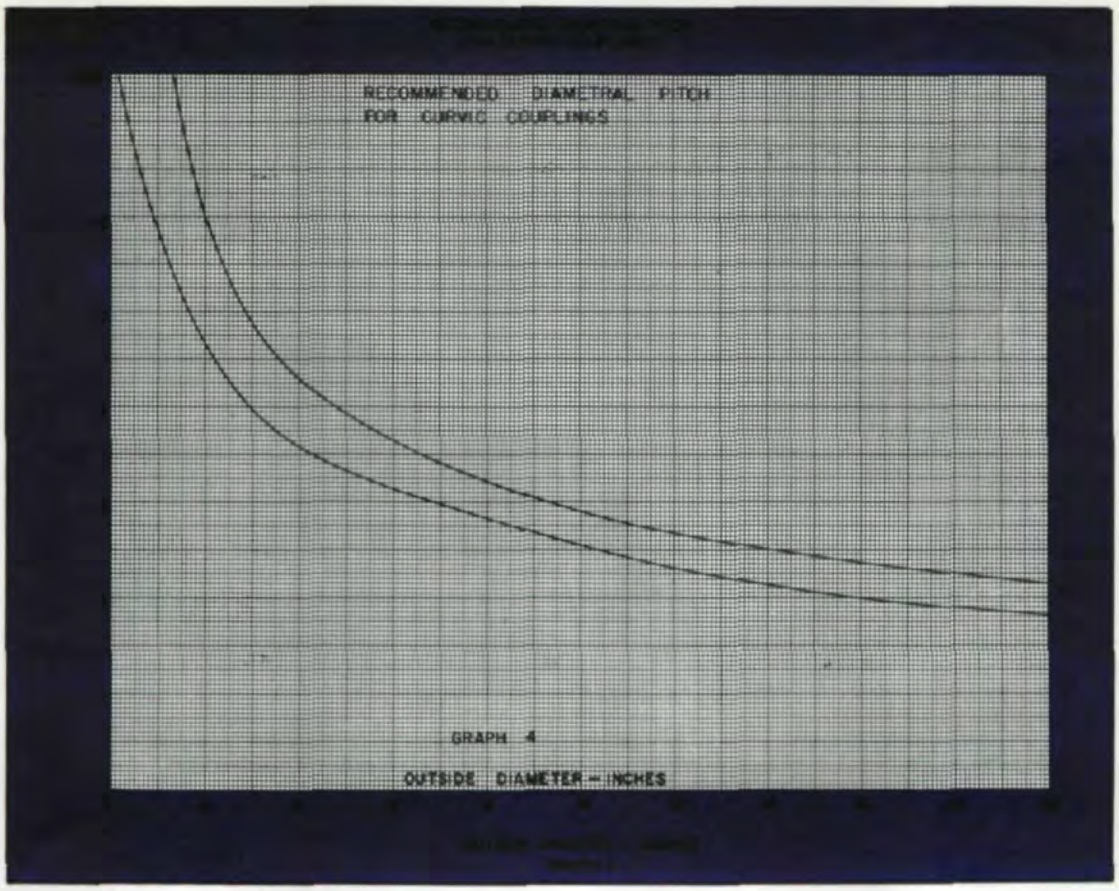
RECOMMENDED DIAMETRAL PITCH
FOR CURVIC COUPLINGS
GRAPH 4
OUTSIDE DIAMETER - INCHES

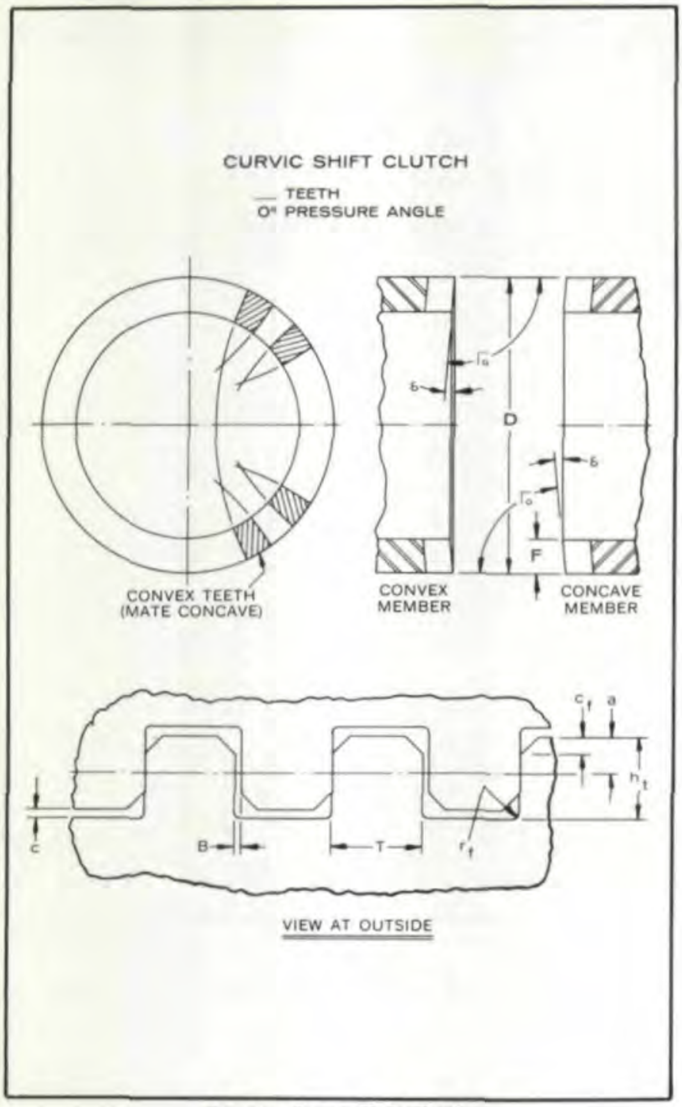

Fig. 16 – Curvic Shift Clutch.

(1) the separating force produced by the action of the torque on the Curvic teeth, (2) the separating force produced by any bending moment on the assembly, and (3) other separating forces, such as those produced by gas pressure, thrust loads, or other external operating characteristics.

The separating force produced by torque is found as follows, neglecting the effect of friction:

$$F_1 = \frac{T}{A} \tan \phi$$

where F_1 = separating force caused by torque
T = torque
A = mean radius of coupling
ϕ = pressure angle

The maximum separating force produced by a bending moment acting on the coupling assembly is

$$F_2 = \frac{5DM}{(D\text{-}F)^2}$$

where M = bending moment, inch lbs.

This maximum separating force produced by a bending moment occurs only at one point on the periphery of the Curvic coupling. The value of separating force drops off on either side of this point in proportion to the distance from the neutral axis. It is assumed that the coupling represents the cross-section of a beam with the neutral axis at the axis of the coupling. The neutral axis may actually be nearer the coupling periphery, but the above choice gives a higher separating force and, thus, a more conservative design approach. After the clamping force is chosen to meet these conditions, the resulting surface stress on the Curvic coupling teeth should be calculated according to the following formula:

$$S_{ec} = \left(\frac{1}{NFh_o} \quad \frac{F_c}{2 \tan \phi} + \frac{T}{A} \right)$$

where S_{ec} = equivalent surface stress, drive side, psi.
N = number of teeth
F = face width, inches
h_o = contact depth, inches
F_o = clamping force, lbs.
T = torque, lbs. inches
ϕ = pressure angle
A = mean radius of coupling, inches

This calculated surface equivalent stress should not exceed the compressive yield strength at the operating temperature of the material being used.

As with any design consideration, it is important that the calculated clamping force be applied to the actual assembly. Where multiple bolts are used, they should all be elongated by the same amount within 1%. To assist the shop in maintaining these values, it is helpful for the designer to provide a convenient means for measuring or gaging the final bolt lengths at assembly. The use of a hollow bolt facilitates assembly by allowing a heating element to be inserted to elongate the bolt a predetermined amount. The nut is then tightened by hand and, after cooling, the required amount of tension is obtained.

When the bolts must pass through the region of the Curvic teeth, it is possible to use a split-face Curvic. This type of coupling has an inner and outer row of teeth separated by a groove for the bolt holes. The same stress formulas are used, with the sum of the two sections of face width inserted for the face width value.

Rotor Design

Turbine and compressor rotors make up the largest proportions of Fixed Curvic Coupling applications at present. Typical construction with multiple clamping bolts is shown in Figs. 2, 3 and 4. Generally, multiple clamping bolts are perferred for rotors where the coupling outside diameter is greater than 10 inches. Satisfactory rotors have been built with a single through bolt, but this requires a heavier section in the end member to transfer the clamping force from the region of the bolt to the region of the Curvic coupling. Also, a single bolt tends to be affected by bending moments on the rotor, whereas multiple bolts simply adjust to changes in the preload as the assembly rotates.

Any suitable material can be used for turbine and compressor rotors since the Curvic Coupling Grinders can be provided with the optimum automatic grinding cycle for the material chosen. To date, all varieties of heat-resistant alloys, stainless steel, alloy steel, stellite, aluminum, aluminum bronze, and titanium have been ground satisfactorily.

The use of unlike materials in mating Curvic coupling rotor discs creates a condition where the two couplings tend to expand at different rates as the temperature increases. The standard Curvic tooth with an average amount of lengthwise curvature has been found to provide sufficient locking action for most applications to date.

If a special design requirement makes it necessary to permit relative movement, the Curvic coupling can be designed with teeth which have a "half-barrel" shape.

This removes the radial restraining force and permits one member to expand with respect to the other. Since the expansion maintains the same tooth angle, regardless of diameter, the centering action of the Curvic coupling remains unchanged. It should be noted, however, that the clamping force exerts a very strong fractional force which tends to resist relative movement, regardless of the tooth shape.

Many aircraft rotor designs are composed of extremely light-weight sections which require additional locking action in the Curvic teeth to resist the effect of centrifugal force. Here, a smaller diameter grinding wheel can be used to provide more lengthwise curvature on the teeth. Some designs have separate light-weight spacers between the discs and these spacers are supported against centrifugal force only through the Curvic coupling teeth. A variation of the "half-barrel" shaped tooth is used in such cases to provide extra resistance to this centrifugal force which is always acting in the same relative direction. When the amount of the relative centrifugal force is known, the included angle made by lines tangent to the two sides of a tooth can be determined to provide the maximum locking action, while keeping the separating force produced by this action within safe limits.

A turbine or compressor rotor which requires a series of different Curvic coupling diameters to fit a tapering rotor configuration can often be made so that three or four diameters can be taken from the same basic coupling development. In this way, fewer developments are required with a resulting saving in machine set-up time and tooling. In the case of the split-face coupling, these Curvic coupling teeth must have special calculations for balanced tooth area.

When cooling air is required to be transmitted to the interior of a rotor, it is usually possible to provide extra clearance at the roots of the Curvic coupling teeth. By using the addendum and chamfer values found from the alternate tooth proportions and the whole depth value from the standard tooth proportions, a practical amount of additional clearance can be determined. For face widths below the maximum limit, it is often practical to exceed the standard depth to obtain more clearance area. The removal of teeth from a Curvic coupling to provide cooling air passage should be avoided if possible.

In the opposite case, where the Curvic teeth must be completely sealed to prevent the passage of air, it is possible to machine a narrow circular groove in the face of both members before the Curvic teeth are ground. At assembly, a flexible metallic sealing strip can be inserted in this groove and the members mated to form a seal. It is important that the sealing strip be flexible enough so that no centering action will take place to oppose the centering action of the Curvic coupling.

The number of Curvic teeth should be made an even multiple of the number of clamping bolts to make it possible to assemble the parts of several different mesh points. The usual practice for rotor assembly is to first balance the individual discs and to mark the heavy point on each disc. At assembly, the heavy points are placed 180° apart on each succeeding disc to obtain the best assembled balance.

For best control of runout at the periphery of the disc, the disc diameter before blading should not exceed 2.5 times the Curvic coupling outside diameter.

Design Example – Rotors

Suppose it is required to design a Curvic coupling for an aircraft compressor rotor to transmit a maximum torque of 340,000 lbs. inches. The design configuration requires that the Curvic coupling outside diameter should be from 10.5" to 11" with a face width of 0.375". (The use of the formula

$$D = \sqrt[3]{\frac{T}{1310}}$$

indicates that a much smaller coupling could be used to carry the load but other design factors have determined the size.)

The material selected has a yield strength of 100,000 psi. at operating temperature and an ultimate strength of 150,000 psi.

We calculate the stresses for a 10.875" O.D. and a .375" face width, and a pressure angle of 30°. From Graph 4 we find that the suggested diametral pitch range for this diameter is from 4.9 to 5.6. We will choose 54 teeth for this example.

$$P_d = \frac{N}{D} = \frac{54}{10.875} = 4.97$$

$$^*h_t = \frac{.616}{P_d} = \frac{.616}{4.97} = .124''$$

$$^*c = \frac{.070}{P_d} = \frac{.070}{4.97} = .014''$$

$$^*c_f = \frac{.063}{P_d} = \frac{.063}{4.97} = .014''$$

$$A = \frac{D-F}{2} = \frac{10.875-.375}{2} = 5.25$$

$$h_o = (h_t - c - 2c_f) = .124 - .014 - 2(.014) = .082$$

$$s_s = \frac{T}{\pi A^2 F} = \frac{340{,}000}{\pi \times (5.25)^2 \times .375} = 10{,}470 \text{ psi.}$$

$$s_c = \frac{T}{AFNH_o} = \frac{340{,}000}{5.25 \times .375 \times 54 \times .082} = 39{,}000 \text{ psi.}$$

$$s_{ec} = \frac{1}{NFh_o}\left(\frac{F_c}{2\tan\phi} + \frac{T}{A}\right)$$

$$= \frac{1}{54 \times .375 \times .082}\left(\frac{150{,}000}{2 \times .57735} + \frac{340{,}000}{5.25}\right)$$

$$= .602\ (129{,}900 + 64{,}800) = .602\ (194{,}700) = 117{,}200 \text{ psi}$$

*Use value to the nearest even .002".

Semi-Universal Curvic Couplings

Having chosen the Curvic coupling diameter from Graph 2 or formula and the number of teeth, the tooth loads on this type of coupling should be checked according to the following formula:

$$F_3 = \frac{T}{2AF}$$

where F_3 = tooth loading, lbs. per 1 inch face.
A = mean radius of coupling, inches.
F = face width, inches.

For satisfactory operations, "F_3" should not exceed 2500 lbs. per 1" face width when the coupling teeth are made of case-hardened steel with a minimum hardness of 60 Rockwell "C".

Successful operation of the semi-universal Curvic coupling is largely dependent on the profile curvature which is introduced on the convex member. The pressure angle is always 0° at the pitch plane. When properly designed, this curvature keeps the tooth contact safely positioned within the boundaries of the tooth surface. It also increases the number of teeth in contact at any instant. The load calculation, however, is based on having two teeth in contact. Angular misalignment must not exceed 2°. Parallel offset of the shafts is limited to *one-half the amount of backlash.*

To determine the required profile curvature on the convex member, calculate the value of ΔS_p which is the bearing shift above or below center on the two diametrically opposite teeth in contact.

$$\Delta S_p = \frac{A \sin \Delta\Sigma}{2 \sin \Theta_o}$$

where ΔE = angular misalignment
A = mean radius of coupling

$$\tan 2\Theta_o = \frac{A}{R_p}$$

R_p = profile radius of cutter

It must be remembered that ΔS_p represents the shift of the center of the tooth contact and should not be permitted to travel to the edge of the tooth. The height of profile contact can be found as follows:

$$h_p = \sqrt{0.002\ R_p}$$

From these calculations, the addendum is obtained as follows:

$$a = \Delta S_p + \frac{h_p}{2} + c_t + .015''$$

The clearance at the roots of the teeth must be at least as large as the fillet radius plus the axial component produced by the angular misalignment plus the amount of axial freedom required in the coupling. The entire tooth design must be executed by trial. As a first assumption, choose a profile radius equal to the cutter radius. If the required tooth depth is greater than 1.25 times the circular tooth thickness at the outside diameter, another trial should be made with a different profile radius or cutter diameter.

A typical Semi-Universal Curvic coupling tooth application is shown in Fig. 10. Suitable arrangements must be made for lubricating the assembled unit. An enclosed design can be packed with grease or pressure lubricated.

Shift and Overload Clutches

The number of tooth shapes which can be designed for shift and overload clutches is practically unlimited, and it will only be possible to outline the basic design procedure.

In general, shift clutches can be considered in three categories: (1) clutches having 0° or negative pressure angles, (2) clutches having 10° or positive pressure angles and (3) saw-tooth clutches.

Overload clutches fall primarily in the second category, with pressure angles usually in the range of 30° or 45°, and some overload clutches are in the form of saw-tooth clutches. Special chamfers and helical surfaces can be added to the teeth of these three basic types.

The layout form for a Curvic shift clutch with 0° pressure angle is shown in Fig. 16. A typical clutch of this type is shown in Fig. 11. This type of shift clutch produces no axial thrust and, in fact, requires a substantial force to disengage it when operating under load in order to overcome the effect of friction. If vibration exists during operation and if there are slight errors in concentricity and parallelism when the members are assembled, there exists a tendency for the clutch to slowly work out of engagement during operation. To overcome this possibility, a clutch with a slight negative pressure angle is often employed, usually from 2° to 5° negative, and this creates a thrust force working to keep the coupling members engaged.

To facilitate disengagement of the clutch members, as well as engagement, a pressure angle of 10° is often used. Experience has shown that the separating force with a 10° pressure angle is approximately equal to the force of friction so that only a light load on the shifter mechanism is needed

(continued on page 48)

CLASSIFIED

Rates: Classified Display—$100 per inch (minimum 3") Type will be set to advertiser's layout or *Gear Technology* will set type at no extra charge. **Word Count:** 35 characters per line, 7 lines per inch.

Payment: Full payment must accompany classified ads. Mail copy to *Gear Technology*, P.O. Box 1426, Elk Grove Village, IL 60007. **Agency Commission:** No agency commission on classifieds.

Closing date: Ads must be received by the 25th of the month, two months prior to publication. **Acceptance:** Publisher reserves the right to accept or reject classified advertisements at his discretion.

HELP WANTED

SUBCONTRACT WORK

FOR SALE

There's still time . . .
closing date for a classified ad in the Jan./Feb. issue is
Nov. 25th

KINEMATIC ANALYSIS OF ROBOTICS . . .

(continued from page 13)

References

1. ALLEN, R. R., "Multiport Models for the Kinematic and Dynamic Analysis of Gear Power Transmission," ASME *Journal of Mechanical Design*, Vol. 101, No. 2, Apr. 1979, pp. 258-267.
2. ANONYMOUS, "Bevel Gears Make Robot's 'Wrist' More Flexible," *Machine Design*, Vol. 54, No. 18, Aug. 12, 1982, p. 55.
3. BUCHSBAUM, F., and FREUDENSTEIN, F., "Synthesis of Kinematic Structure of Geared Kinematic Chains and Other Mechanisms," *J. Mechanisms and Machine Theory*, Vol. 5, 1970, pp. 357-392.
4. DAY, C. P., AKEEL, H. A., and GUTKOWSKI, L. J., "Kinematic Design and Analysis of Coupled Planetary Bevel-Gear Trains," ASME *Journal of Mechanisms, Transmissions, and Automation in Design*, Vol. 105, No. 3, Sept. 1983, pp. 441-445.
5. DIMENTBERG, F. M., "Determination of the Positions of Spatial Mechanisms," (Russian), *Izdat. Akad. Nauk*, Moscow, 1950.
6. FREUDENSTEIN, F., "An Application of Boolean Algebra to the Motion of Epicyclic Drives," ASME *Journal of Engineering for Industry*, Vol. 93, 1971, pp. 176-182.
7. FREUDENSTEIN, F., and YANG, A. T., "Kinematics and Statics of a Coupled Epicyclic Spur-Gear Train," *J. Mechanisms and Machine Theory*, Vol. 7, 1972, pp. 263-275.
8. MERRITT, H. E., *Gear Trains*, Pitman and Sons, London, 1947.
9. POLDER, J. W., *A Network Theory of Variable Epicyclic Gear Trains*, Eindhoven, Greve Offset, 1969.
10. YANG, A. T., and FREUDENSTEIN, F., "Mechanics of Epicyclic Bevel-Gear Trains," *ASME Journal of Engineering for Industry*, Vol. 95, 1973, pp. 497-502.

The authors are grateful to the General Motors Research Laboratories for the support of this research through a grant to Columbia University.

This article was previously presented at the ASME Design Engineering Technical Conference, October 1984. Paper No. 84-Det-22.

CURVIC COUPLING DESIGN . . .

(continued from page 46)

to keep the clutch teeth in engagement or to move them out of engagement. Higher pressure angles are often used for shift clutches to obtain a proportionately wider space between the toplands of teeth for easy engagement.

The tooth contact of non-generated clutch teeth with positive pressure angle will move very quickly to the edge of the tooth at the heel as the clutch is disengaged under load. To obtain proper tooth contact at all depths of engagement, a generated helical surface should be used. For the great majority of small clutches which shift under load, however, it is entirely satisfactory to design both members with identical convex teeth. When both members are convex, the localized tooth contact remains safely positioned on the surface of the teeth at all depths of engagement thus approximating the action of a helical surface.

Since this localized tooth contact travels from toe to heel as the teeth are disengaged, the amount of this bearing shift should be calculated.

$$\Delta S_L = \frac{h_o}{2} \tan \phi \frac{r_c}{A}$$

where ΔS_L = bearing shift lengthwise on the tooth

h_o = contact depth

ϕ = pressure angle

r_c = cutter radius

A = mean radius of coupling

This calculated amount of bearing shift should be compared with the available face width as follows:

$$\Delta S_L = F - \tfrac{1}{2}\sqrt{\frac{r_c}{1000}}$$

where F = face width

The shift clutch diameter which has been determined in a previous section should be checked according to the formula below. This applies to case-hardened teeth which shift under load and the calculated stress should not exceed 150,000 psi. maximum at operating temperatures.

$$s_c = \frac{0.9T}{AF\, h_o}$$

where s_c = surface stress, psi.

T = torque, lbs. inches

A = mean radius of clutch, inches

F = face width, inches

h_o = contact depth

For clutches which shift under stationary no-load conditions, the surface stress should not exceed 40,000 psi. for case-hardened steel, as given by the following formula:

$$s_c = \frac{T}{AFN\, h_o}$$

The standard tooth proportions given in an earlier section are suggested for initial use in designing shift and overload clutches.

* * *

MIRROR FINISHING OF TOOTH SURFACES . . .

(continued from page 26)

8. OPITZ, H., and GÜHRING, K., "High Speed Grinding", *Annals of CIRP*, Vol. 16, 1968, p. 61-73.
9. ISHIBASHI, A., "The Characteristic of Circular-Arc-Toothed Cylindrical Gears", *Bull. Japan Soc. Mech. Engrs.*, Vol. 9, No. 33, Feb. 1966, p. 200-208.

The authors express their thanks to Emeritus Profs. A. Wakuri and T. Ueno, Kyushu University, for their encouragement. They are also indebted to the staff of the Machine Shop of the Faculty of Science and Engineering, Saga University, for making the gear grinder used in this investigation.

This article was previously presented during the November, 1984 ASME Technical Conference. Paper no. 84-DT-153.